

Molecular Characterization of Phosphatidylserine Decarboxylase 1 from Yeast

Master thesis

accomplished by

Stefanie M. Horvath

Institute of Biochemistry
Graz University of Technology

Supervisor: Ao. Univ.-Prof. Dipl.-Ing. Dr.techn. Günther Daum

Graz, November 2012

I'd like to express my gratitude to Ao. Univ.-Prof. Dipl.-Ing. Dr. techn. Günther Daum for giving me the possibility to work in his group. Thus, I gained invaluable experiences, further knowledge of biochemical approaches and laboratory work routine. Special thanks go to my sister Dipl.-Ing. Susanne Horvath for her never-ending patience, her unfailing efforts to refer her own knowledge to me and her excellent support throughout the master thesis and my entire studies. Last but not least I also want to thank my parents and boyfriend Mario for supporting me during the last five years.

Table of content

Table of content	I
Abstract	IV
Zusammenfassung.....	V
Abbreviation	VI
1 Introduction.....	1
1.1 Glycerophospholipids of the yeast <i>Saccharomyces cerevisiae</i>	1
1.1.1 General aspects and structural features of glycerophospholipids.....	1
1.1.2 Biosynthesis and functions of glycerophospholipids.....	3
1.1.2.1 Phosphatidic acid.....	3
1.1.2.2 Phosphatidylinositol and phosphoinositides	6
1.1.2.3 Phosphatidylglycerol and cardiolipin	8
1.1.2.4 Aminoglycerophospholipids.....	9
1.1.2.4.1 Phosphatidylserine (PS).....	10
1.1.2.4.2 Phosphatidylethanolamine (PE)	10
1.1.2.4.3 Phosphatidylcholine (PC).....	13
1.2 Mitochondria	14
1.2.1 Phospholipids of mitochondria	14
1.2.2 General and structural aspects of mitochondria.....	16
1.2.3 The mitochondrial protein import machinery	18
1.2.3.1 Transport to mitochondria: targeting sequence and cytosolic chaperons.....	18
1.2.3.2 The TOM complex	20
1.2.3.3 The TIM complex	20
1.3 Phosphatidylserine decarboxylase 1 in yeast.....	21
1.3.1 General aspects of phosphatidylserine decarboxylases.....	21
1.3.2 Characteristic sequence motifs of phosphatidylserine decarboxylase 1	22
1.3.3 Biogenesis and processing of phosphatidylserine decarboxylase 1.....	24
1.3.4 Enzymatic properties of phosphatidylserine decarboxylase 1.....	26
1.1.3.4.1 Enzymology of phosphatidylserine decarboxylases.....	26
1.1.3.4.2 Regulation of phosphatidylserine decarboxylase activity.....	28
2 Aims of the thesis	29

3 Materials and Methods	30
3.1 Strains and culture conditions.....	30
3.1.1 <i>E. coli</i> strains and culture conditions	30
3.1.2. <i>Saccharomyces cerevisiae</i> strains and culture conditions.....	31
3.2 Plasmids and strain construction.....	33
3.2.1 Overlap-extension PCR	33
3.2.2 Ligation and transformation in <i>E. coli</i>	37
3.2.3 TELT method: a quick method for plasmid isolation	39
3.2.4 Restriction	40
3.3 Plasmid transformation in the yeast <i>Saccharomyces cerevisiae</i>	40
3.3.2 Lithium Acetate Transformation.....	40
3.3.3 Colony-PCR.....	42
3.4 Organelle preparation – Isolation of mitochondria.....	43
3.4.1 Growth of <i>Saccharomyces cerevisiae</i> BY4741 and various mutant strains.....	43
3.4.2 Spheroplast preparation	43
3.4.3 Isolation of mitochondria.....	44
3.5 Analytical methods	45
3.5.1 Protein Analyses.....	45
3.5.1.1 Protein precipitation and quantification.....	45
3.5.1.2 SDS-PAGE.....	46
3.5.1.3 Western Blot analysis	48
3.5.2 Submitochondrial localization of proteins and solubility studies.....	50
3.5.2.1 Submitochondrial localization studies	50
3.5.2.2 Carbonate extraction.....	51
3.5.3 Phospholipid analyses.....	52
3.5.3.1 Lipid extraction from mitochondria and homogenate fractions	52
3.5.3.2 Lipid analysis by two dimensional thin layer chromatography.....	53
3.5.3.3 Phospholipid determination.....	54
3.5.4 Enzymatic activity assay	54
4 Results	56
4.1 Dissection of Psd1 into specific domains.....	56
4.2 Submitochondrial localization of Psd1 Δ IM2, Psd1 Δ IM1+2 and Psd1 Δ SRS	59
4.3 Psd1 is anchored to the inner mitochondrial membrane by IM1	62

4.4 Functionality of wild type Psd1 and Psd1 variants.....	64
4.4.1 Impaired Psd1 processing causes loss of enzymatic activity.....	64
4.4.2 Phospholipid distribution of wild type and Psd1 variants.....	66
5 Discussion.....	69
7 References.....	74
8 Curriculum vitae.....	80

Abstract

In yeast, phosphatidylserine decarboxylase 1 (Psd1) is the major enzyme catalysing the formation of phosphatidylethanolamine (PE) from phosphatidylserine (PS). Psd1 is composed of an α - and a β -subunit and located to the intermembrane space and the inner mitochondrial membrane, respectively. Within the 46 kDa β -subunit, two possible transmembrane domains IM1 and IM2 were predicted to anchor the enzyme to the inner mitochondrial membrane. To get more information about the mechanism(s) targeting Psd1 to the inner mitochondrial membrane/intermembrane space we constructed a series of Psd1 variants lacking IM1, IM2 or both transmembrane domains. Moreover, we deleted a domain within the α -subunit which is predicted to be the substrate recognition site in analogy to mammalian Psd. For detailed molecular characterisation of Psd1 processing/maturation, mitochondria of the respective mutant strains were isolated and analysed. Phospholipid analysis and enzyme assays revealed a requirement for IM2 not only for Psd1 function and processing, but also for correct targeting to the inner mitochondrial membrane. Although deletion of IM1 does not inhibit cleavage of Psd1 into α - and β -subunits, a mislocalization of both non-identical subunits to the matrix side of the inner mitochondrial membrane was observed. We conclude that IM1 serves as a membrane anchor for the β -subunit, whereas IM2 targets the enzyme to the inner mitochondrial membrane. Moreover, IM2 may also contribute to Psd1 maturation by formation of α - and β -subunits. We could also hypothesize that the potential substrate recognition site within the α -subunit is not only involved in recognition of phosphatidylserine, but also in Psd1 processing and stability.

Zusammenfassung

Phosphatidylserindecaboxylase 1 ist ein mitochondriales Enzym und verantwortlich für den Hauptanteil der Phosphatidylethanolamine Biosynthese in *Saccharomyces cerevisiae*. Psd1 besteht aus zwei Untereinheiten, α und β , die im Intermembranraum und der inneren mitochondrialen Membran lokalisiert sind. Innerhalb der 46 kDa β -Untereinheit befinden sich zwei vorhergesagte Transmembrandomänen, IM1 und IM2, die für die Verankerung der β -Untereinheit in die innere mitochondriale Membran verantwortlich sein sollen. Um mehr Informationen über diese potentiellen Transmembranregionen zu erhalten und einen besseren Einblick in die mitochondrialen Targeting-Mechanismen von Psd1 zu bekommen, wurden verschiedene Psd1 Mutanten, in denen entweder die erste, die zweite oder beide möglichen Transmembrandomänen deletiert wurden, kloniert. Außerdem wurde eine Psd1 Mutante ohne Substraterkennungssequenz (SRS) generiert. Für eine detaillierte molekulare Charakterisierung der Prozessierung und Reifung von Psd1 wurden Mitochondrien jener Mutanten isoliert und analysiert. Phosphatbestimmungen und Enzym-Assays zeigten, dass die zweite Transmembrandomäne (IM2) nicht nur für die korrekte Funktion und Prozessierung von Psd1, sondern auch für das Psd1 Targeting zur inneren mitochondrialen Membran verantwortlich ist. Obwohl die Deletion der ersten Transmembranregion (IM1) keine Inhibierung der Spaltung von Psd1 in seine α - und β -Untereinheit bewirkte, führte sie zu einer Fehllokalisierung beider Untereinheiten an die Matrixseite der inneren mitochondrialen Membran. Anhand der erhaltenen Daten konnten den einzelnen Psd1 Domänen spezifische Funktionen zugeordnet werden. IM1 fungiert als Membrananker, welcher das Enzym über die β -Untereinheit an die innere mitochondriale Membran bindet. Im Gegensatz dazu ist IM2 an der Prozessierung und dem mitochondrialen Targeting von Psd1 beteiligt. Die Substraterkennungssequenz ist nicht nur für die Prozessierung von Psd1, sondern auch für die Stabilisierung des Enzyms verantwortlich.

Abbreviation

AGAT	1- acyl glycerol 3-phosphate acyltransferase
Ale1	acyltransferase for lysophosphatidylethanolamine
CDP-DAG	cytidindiphosphate diacylglycerol
Cho	choline
Cho1	phosphatidylserine synthase
CL	cardiolipin
C-terminus	carboxyl terminus
Da	Dalton
DAG	diacylglycerol
DGPP	diacylglycerol pyrophosphate
DHAP	dihydroxyacetone phosphate
DHAPAT	dihydroxyacetone phosphate acyltransferase
DNA	deoxyribonucleic acid
DMPE	dimethylphosphatidylethanolamine
dNTP	deoxyribonucleotide triphosphate
dmp	disintegrations per minute
DTT	dithiotreitol
EDTA	ethylenediaminetetraacetic acid
ELM	endogenous lysolipid metabolism
Etn	ethanolamine
GAT	glycerol 3-phosphate acyltransferase
Gro-PE	glycerol-phosphoethanolamine
h	hour
hsDNA	herring sperm deoxyribonucleic acid
IM	transmembrane domain
Ins	inositol
kb	kilo base
LPA	lysophosphatidic acid
LPL	lysophospholipids
LSC	liquid scintillation counting
MeOH	methanol

Min	minute
mM	millimolar
NADPH	nicotinamide adenine dinucleotide phosphate
OD	optical density
PA	phosphatidic acid
PAGE	polyacrylamide gel electrophoresis
PCR	polymerase chain reaction
PEG	polyethylene glycol
PLB	phospholipase B
PMSF	phenylmethylsulfonylfluoride
Psd1	phosphatidylserine decarboxylase 1
Psd2	phosphatidylserine decarboxylase 2
PC	phosphatidylcholine
PE	phosphatidylethanolamine
PG	phosphatidylglycerol
PI	phosphatidylinositol
PS	phosphatidylserine
rpm	revolutions per minute
SDS	sodiumdodecylsulfate
sec	second
Ser	serine
SRS	substrate recognition site
TAG	triacylglycerol
TBE	tris-borate-EDTA-electrophoresis buffer
TBS	tris-buffered saline
TCA	trichloroacetic acid
TE	tris-EDTA buffer
TEMED	tetramethylethylene diamine
Tris	trihydroxymethylaminomethane
v/v	volume/volume
w/v	weight/volume

1 Introduction

1.1 Glycerophospholipids of the yeast *Saccharomyces cerevisiae*

1.1.1 General aspects and structural features of glycerophospholipids

Lipids belong to a major class of biological molecules found in all cells. The class of molecules is defined by their large hydrophobicity and solubilisation in organic solvents (Voet et al., 2008). Moreover, lipids are defined as molecules that are created entirely or at least partially by carbanion-based condensations of thioesters (for example fatty acids) and by carbocation-based condensations of isoprene units (for example sterols). Generally, lipids have been divided into two different subclasses, namely simple and complex groups. Hydrolysis of simple lipids, like fatty acids or sterols, gives rise to two products, whereas complex lipids yield three or more hydrolysis products (Fahy et al., 2005).

Glycerophospholipids, also known as phospholipids, belong to the group of complex lipids consisting of a glycerol-3-phosphate backbone esterified with fatty acids (Figure 1). Saturated fatty acids are usually linked to the *sn*-1 position of the glycerol-3-phosphate backbone, whereas unsaturated fatty acids are predominantly found in the *sn*-2 position. The most abundant fatty acids in yeast are palmitic acid (C-16:0), palmitoleic acid (C-16:1), stearic acid (C-18:0) and oleic acid (C-18:1) whereas myristic acid (C-14:0) and C-26 fatty acids are only detected in minor amounts. The *sn*-3 position of the glycerol backbone is esterified with a phosphate, which is linked by one of its hydroxyl groups to a polar head group (Daum et al., 1998). Thus, glycerophospholipids are amphiphilic molecules with polar phosphoryl-X heads and nonpolar aliphatic tails, formed by the fatty acids in the *sn*-1 and *sn*-2 position of the glycerol backbone (Voet et al., 2008).

The nature of the polar head group is not only important for classifying the various phospholipids, but also for the interaction with proteins. Acid head groups of phosphatidic acid, phosphatidylserine, phosphatidylinositol and phosphatidylglycerol for instance are capable of electrostatic interactions with positively charged protein residues (Nebauer et al., 2004).

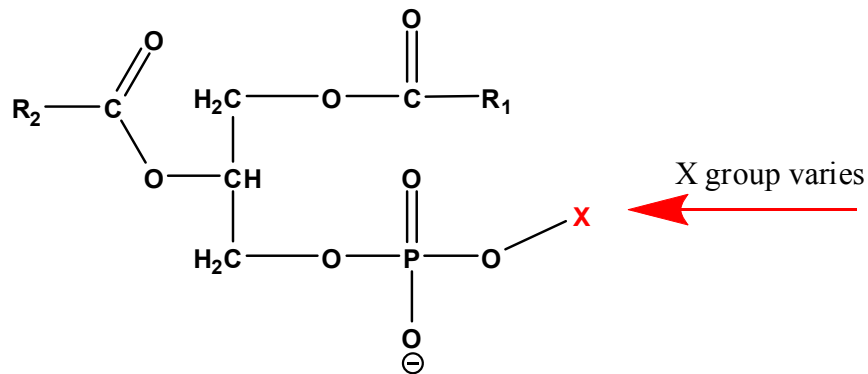


Figure 1: Structure of glycerophospholipids. Glycerophospholipids consist of a glycerol-3-phosphate backbone esterified with fatty acids. The X group of the phosphoryl-X heads at the *sn*-3 position can be an ethanolamine, a choline, a serine, a glycerol, a phosphatidylglycerol, a *myo*-inositol or a water molecule.

Functions of glycerophospholipids are manifold. They are regarded as primary and most essential components of biological membranes, which serve as diffusion barriers between the interior of the cell and its environment as well as between the lumen of organelles and the cytosol. Beside their role in separating cellular compartments, biological membranes harbour specific proteins that catalyze selective transport processes of molecules or act as enzymes in metabolic and regulatory pathways. Moreover, biological membranes contain receptors that participate in recognition processes (Daum et al., 1998).

Most biological membranes display a bilayer organization of lipids. Despite this relative simple structural arrangement of lipid molecules, biological membranes encompass an extra level of complexity through asymmetric composition of each monolayer. The inner lipid monolayer of most eukaryotic membranes for example is composed of phosphatidylserine

and phosphatidylethanolamine, whereas the outer monolayer harbours most of the phosphatidylcholine and sphingomyelin. Generally, lipids which exhibit a cylindrical shape with an equal head group to hydrocarbon area assemble into lipid bilayers like the major bilayer forming lipid phosphatidylcholine. In contrast lipids with small head groups and cone like shapes such as phosphatidylethanolamine and cardiolipin are non-bilayer forming lipids (Hafez and Cullis, 2001).

Biosynthesis of different phospholipids is not restricted to a single cellular compartment. Thus, transport and sorting of lipids to their intracellular destination are important processes which must be coordinated with lipid metabolic pathways to ensure maintenance of the overall lipid homeostasis. Investigation of subcellular fractions assigned an unique composition of glycerophospholipids to each organelle. Phosphatidylglycerol and cardiolipin are enriched in mitochondrial membranes, where they play an essential role in respiration. In contrast, phosphatidylcholine and phosphatidylethanolamine are considered as bulk phospholipids and as constitutes of all membranes (Nebauer et al., 2004). Growth phases and culture conditions influence the lipid composition of the cell. When *S. cerevisiae* cells enter the stationary growth phase, triacylglycerols accumulate at the expense of total phospholipid synthesis (Homann et al., 1987).

1.1.2 Biosynthesis and functions of glycerophospholipids

1.1.2.1 Phosphatidic acid

Phosphatidic acid (PA) is a key intermediate of glycerophospholipid biosynthesis in the yeast *S. cerevisiae* (Athenstaedt and Daum, 1999).

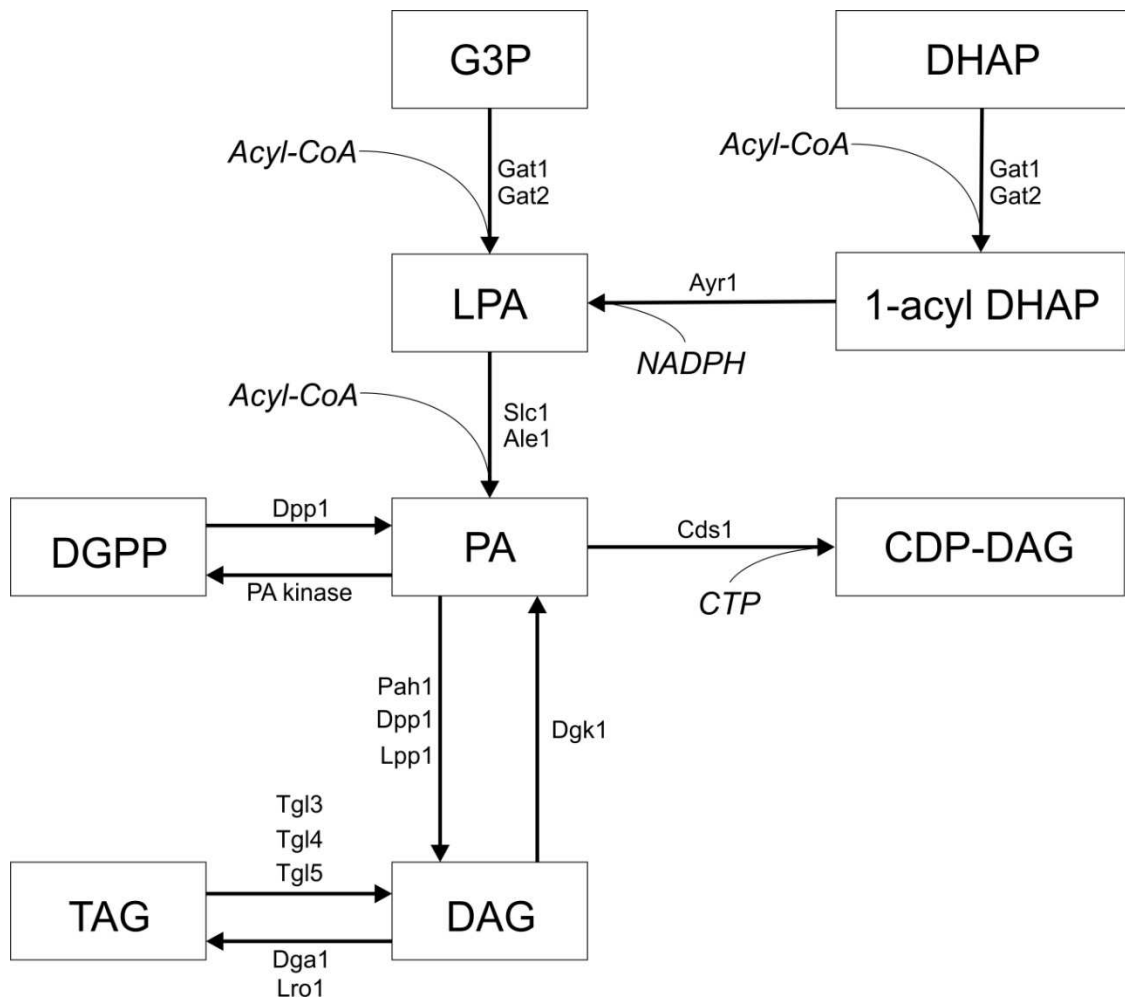


Figure 2: Biosynthesis and breakdown of phosphatidic acid in yeast

PA is generated through two acylation pathways using either glycerol-3-phosphate (G3P) or dihydroxyacetone phosphate (DHAP) as initial substrates (Figure 2). In the first pathway, G3P is acylated by G3P acyltransferase (GAT) at the *sn*-1 position. The generated lysophosphatidic acid (LPA, 1-acyl G3P) is then subjected to a second acylation step, in which lyso-PA acyltransferases (Slc1, Ale1) catalyzes the conversion of LPA to PA. In the second pathway, DHAP is first converted to 1-acyl dihydroxyacetone phosphate by DHAP acyltransferases (Gat1, Gat2) and subsequently reduced to LPA in a NADPH-dependent reaction catalyzed by 1-acyl DHAP reductase (Ayr1). Finally, LPA is acylated to PA (Athenstaedt and Daum, 1999; Rajakumari et al., 2008; Pagac et al., 2011).

Beside *de novo* synthesis via the two acylation pathways, PA can also be formed by alternative biosynthetic routes. One possible route is the phosphorylation of diacylglycerols (DAG) by the diacylglycerol kinase Dgk1 (Fakas et al., 2011). DAG is generated either *via* lipolysis of triacylglycerols, catalyzed by triacylglycerol lipases Tgl3, Tgl4 and Tgl5, or hydrolysis of glycerophospholipids by phospholipase C. In a second route, PA is derived from the hydrolysis of glycerophospholipids, which is catalyzed by phospholipase D. Furthermore, PA formation comprises dephosphorylation of diacylglycerol pyrophosphate (DGPP) *via* DGPP phosphatase (Dpp1) with DGPP generated by phosphorylation of PA (Athenstaedt and Daum, 1999; Rajakumari et al., 2008).

The highest specific activity of G3P acylating enzymes was found in lipid droplets (Christiansen et al., 1987). Moreover, three acyltransferases were identified. Gat1, present in microsomes as well as in lipid droplets, Gat2/Sct1, which is located to microsomes and displays overlapping substrate specificities for G3P and DAPH and a third acyltransferase, which is found in mitochondria and prefers DHAP as precursor (Athenstaedt and Daum, 1999). The enzyme linking the G3P and the PHAP pathway of PA formation, 1-acyl DHAP reductase (ADR, Ayr1), is present in lipid droplets and the endoplasmic reticulum, but not in mitochondria. 1-acyl DHAP is formed in mitochondria and has to be transported to a site of ADR activity for the conversion to LPA. The translocation of the largely water soluble 1-acyl DHAP to the site of conversion may be achieved either by diffusion or by membrane contact between ER and mitochondria *via* mitochondria associated membranes (Nebauer et al., 2004).

PA functions as general precursor of all glycerolipids and plays an important role in the lipid metabolism of yeast. The activation of PA with CTP by a CDP-DAG synthase (Cds1) gives rise to CDP-DAG, which serves as precursor for phosphatidylinositol, phosphatidylglycerol,

cardiolipin, phosphatidylserine, phosphatidylethanolamine and phosphatidylcholine. Moreover, Pah1 a Mg^{2+} -dependent phosphatidate phosphatase (PAP), which belongs to the PAP1 group of enzymes, catalyzes dephosphorylation of PA yielding DAG, which is used as a precursor for aminoglycerolphospholipids synthesis *via* the Kennedy pathway. Additionally, diacylglycerols formed from PA by PAP or alternative pathways can be converted to TAG in another acylation step (Sorger and Daum, 2003; Rajakumari et al., 2008).

In addition, PA and DAG also function as messenger molecules and are recognized as regulators of membrane traffic. The cellular concentration of PA is subjected to strict balancing because changes of the PA level result in cellular dysfunction. DAG destabilizes the membrane bilayer, promotes membrane fusion and decreases the spontaneous curvature of the membrane. These effects suggest that DAG is not only involved in membrane stability and integrity but also in vesicle budding and formation (Nebauer et al., 2004).

1.1.2.2 Phosphatidylinositol and phosphoinositides

Phosphatidylinositol (PI) is the third major phospholipid found in yeast membranes. Deficiency in inositol-containing lipids impairs membrane function. PI serves as a precursor in the synthesis of inositol-containing lipids such as di- and triphosphoinositides and several sphingolipids (Fischl and Carman, 1983). Beside its role as essential precursor and membrane phospholipid, phosphatidylinositol is required for synthesis of GPI anchors, such as Gas1 and α -agglutinin (Daum et al., 1998). Biosynthesis of PI (Figure 3) involves the reaction of CDP-DAG and *myo*-inositol catalyzed by PI synthase, which has been localized in mitochondrial and microsomal fractions of the cell (Fischl and Carman, 1983). The precursor inositol is synthesized by cyclization of glucose 6-phosphate to inositol 1-phosphate *via* MI-1-P synthase (Dean-Johnson and Henry, 1989) and subsequent dephosphorylation by inositol 1-P

phosphatase. In yeast, two specific inositol monophosphatases are found, namely Imp1 and Imp2. Both monophosphatases are not essential for growth and inositol biosynthesis under normal or stress conditions. Therefore, hydrolysis of inositol 1-phosphate by non-specific phosphatases might be more important under physiological conditions (Lopez et al., 1999). Beside the endogenous formation of inositol, exogenous inositol can be incorporated into cells by the inositol transporters Itr1 and Itr2 (Nikawa et al., 1991). Phosphorylation of the head group of phosphatidylinositol, *myo*-D-inositol, at D-3, 4 and 5 positions by kinases gives rise to the phosphoinositides PI 3-P, PI 4-P, PI 3,5-P₂ and PIs 4,5-P₂ (Fruman et al., 1998; Toliyas and Cantley, 1999). Phosphoinositides play an important role in signal transduction. They act as precursors for second messengers or directly recruit effector proteins containing phosphoinositide-binding domains, like the pleckstrin homology (PH) domain. Moreover, phosphoinositides are essential for various cellular processes, like cell differentiation, cytoskeletal organization, glucose transport and cell survival (Nebauer et al., 2004).

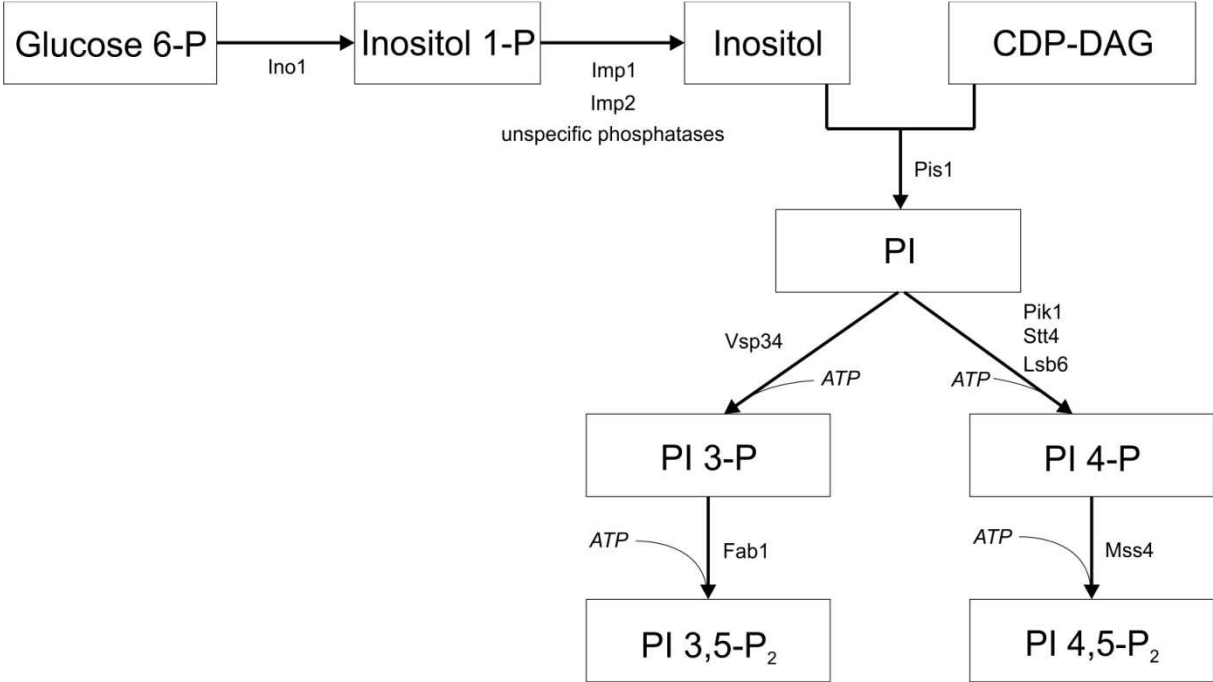


Figure 3: Biosynthesis of phosphatidylinositol and phosphoinositides

1.1.2.3 Phosphatidylglycerol and cardiolipin

Cardiolipin (CL) exhibits a unique dimeric structure with two phosphatidyl moieties linked through a central glycerol group. The CL-synthesizing enzyme, cardiolipin synthase (Crd1), is located to the inner mitochondrial membrane with hydrophobic domains exposed to the matrix side. Thus, CL is synthesized on the matrix side of the inner mitochondrial membrane (Gallet et al., 1997). The first steps of cardiolipin biosynthesis (Figure 4) involve formation of phosphatidylglycerolphosphate (PGP) from CDP-DAG and G3P by PGP synthase Pgs1 and subsequent dephosphorylation of PGP to phosphatidylglycerol (PG) by PGP phosphatase Gep4. Cardiolipin synthase (Crd1) catalyses an irreversible condensation reaction in which CDP-DAG is linked to PG *via* cleavage of a high energy anhydride bond to form premature cardiolipin (CL_p). Remodelling of cardiolipin through deacylation by the phospholipase Cld1, leads to the formation of monolysocardiolipin (MLCL). Reacylation with another fatty acid gives rise to mature CL (CL_M). This reacylation reaction is catalysed by tafazzin (Taz1). Mutations in tafazzin cause the human Barth syndrome, an X-linked cardioskeletal myopathy, which can affect respiratory chain assembly (Gebert et al., 2011).

Although the biosynthesis of CL occurs on the matrix side of mitochondria, CL is predominantly found in the outer leaflet of the inner mitochondrial membrane. However, the amount and transmembrane distribution of CL is subjected to rapid changes upon switch of fermentative to gluconeogenic growth (Gallet et al., 1997; Nebauer et al., 2004). Cells grown on non-fermentable carbon sources like glycerol or lactate, show enhanced proliferation of mitochondria, which leads to an increase of CL in these cells (Tuller et al., 1998; Tuller et al., 1999). CL is not only found in the inner mitochondrial membrane, but also in mitochondrial contact sites, whereas minor amounts could be detected in the outer mitochondrial membrane and peroxisomes (Zinser and Daum, 1995). CL and its precursor

phosphatidylglycerol are components of membranes which form an electrochemical potential for substrate and ATP synthesis. Additionally, CL is known to interact with a large number of mitochondrial proteins, such as ADP/ATP-carriers, cytochrome *bc1* and cytochrome *c* oxidase (Nebauer et al., 2004).

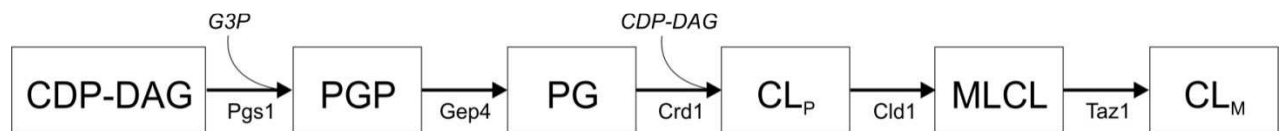


Figure 4: Phosphatidylglycerol and cardiolipin synthesis

1.1.2.4 Aminoglycerophospholipids

Phosphatidylserine (PS), phosphatidylethanolamine (PE) and phosphatidylcholine (PC) belong to the subgroup of aminoglycerophospholipids. Aminoglycerophospholipids are characterized by an amino group as structural element in their head group (Nebauer et al., 2004). Enzymes involved in aminoglycerophospholipids synthesis are topologically segregated: phosphatidylserine synthase is located to the endoplasmic reticulum and the mitochondria associated membrane (MAM) fraction of the ER, phosphatidylserine decarboxylase 1 and 2 are found in mitochondria and a Golgi/vacuole compartment, respectively, whereas phosphatidylethanolamine methyltransferases are located to the endoplasmic reticulum (Achleitner et al., 1995).

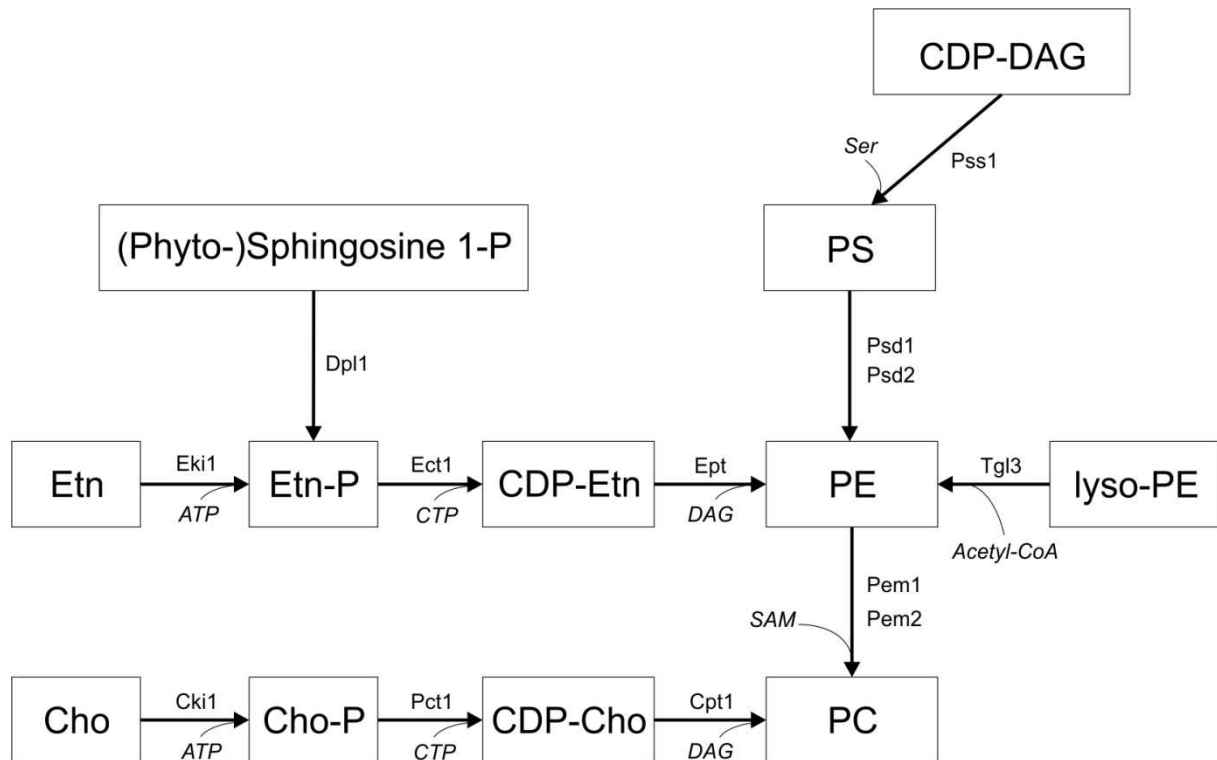


Figure 5: Biosynthesis of aminoglycerophospholipids

1.1.2.4.1 Phosphatidylserine (PS)

In yeast, PS is synthesized from CDP-DAG and serine by phosphatidylserine synthase (Pss1/Cho1), located to the endoplasmic reticulum and related membranes (MAM) (Figure 5). Since mutants lacking the *CHO1* gene do not contain any detectable amounts of PS and are auxotrophic for choline or ethanolamine, it is assumed that Cho1 is the only PS synthase in yeast. Moreover, loss of phosphatidylserine synthesis causes fragmentation of vacuoles, increased susceptibility to Ca^{2+} , Zn^{2+} , Mn^{2+} , L-lysine and L-arginine and a defect in tryptophan transport (Nebauer et al., 2004).

1.1.2.4.2 Phosphatidylethanolamine (PE)

PE can be synthesized *via* several pathways (Figure 5 and 6), including the *de novo* synthesis through decarboxylation of phosphatidylserine by phosphatidylserine decarboxylases (Psd1/Psd2), the CDP-ethanolamine branch of the Kennedy pathway (Daum et al., 1998), and

acyltransferase reactions catalyzed by Ale1 and Tgl3, which acylate lyso-PE to PE (Riekhof et al., 2007; Rajakumari and Daum, 2010).

The major route of PE synthesis is the *de novo* pathway through decarboxylation of phosphatidylserine by phosphatidylserine decarboxylase 1 (Psd1) localized to the inner mitochondrial membrane and intermembrane space (Horvath et al., 2012). PE is also *de novo* synthesized by phosphatidylserine decarboxylase 2 (Psd2), localized to a Golgi/vacuole compartment (Trotter et al., 1995).

An alternative route of PE biosynthesis in yeast is the so-called Kennedy pathway, which is a salvage pathway for cells which are either lacking phosphatidylserine decarboxylase activity or are incapable of synthesizing PS. However, PE synthesis *via* this pathway is only possible if sufficient ethanolamine/choline is either exogenously added to the growth medium or endogenously formed by lipolytic processes. The initial enzymes of this pathway are ethanolamine kinase (Eki1) and choline kinase (Cki1) which exhibit overlapping substrate specificities and are responsible for phosphorylation of ethanolamine and choline. In a second step, the ethanolamine-phosphate (Etn-P) is activated by reaction with cytidyltriphosphate (CTP). This reaction is catalyzed by the ethanolaminephosphate cytidyltransferase (Ect1/Muq1) and gives rise to cytidyldiphosphate ethanolamine (CDP-Etn). In order to gain PE, CDP-Etn is finally linked to diacylglycerol by CDP-ethanolamine:1,2-diacylglycerol ethanolaminphosphotransferase (Ept1). The Kennedy pathway is connected to the sphingolipid catabolism by dihydrosphingosine-phosphate lyase (Dpl1). Dpl1 cleaves phosphorylated sphingosine bases into long chain aldehydes and ethanolaminephosphate (Etn-P) which can serve as substrate for the Kennedy pathway (Birner et al., 2001; Daum et al., 1998).

Another route of PE synthesis is the exogenous lysolipid metabolism (ELM) pathway (Figure 6). In this pathway, PE is formed from lyso-PE by Ale1 (acyltransferase for lyso-PE) which is localized to the mitochondria associated membrane (MAM) fraction. Lyso-PE is imported into the cell through two plasma membrane P-type ATPases, namely Dnf1 and Dnf2 and their non-catalytic β -subunit Lem3. Subsequently, the internalized lyso-phospholipid is rapidly acylated by the acyl-CoA-dependent lyso-PE acyltransferase (Ale1) to PE. Beside acylation by Ale1, PE can also be formed by a catabolic pathway carried out by the ER-localized phospholipase B enzyme (PLB) Nte1 (Riekhof et al., 2007).

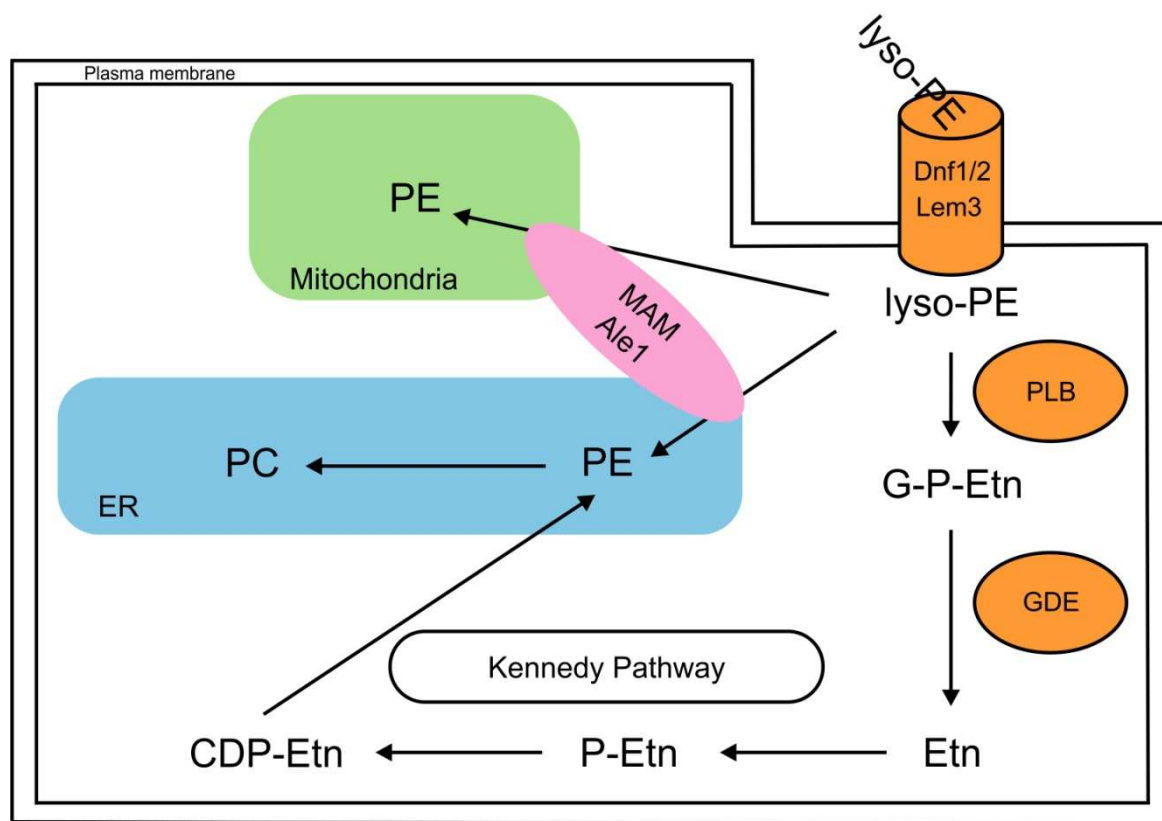


Figure 6: The ELM pathway

Since PE is one of the major membrane phospholipids, and its continuous supply for proper cell growth is crucial. On non-fermentable carbon sources the requirement of PE becomes more stringent than on fermentable carbon sources. Thus, mitochondrial synthesis of PE by Psd1 becomes paramount. Under non-fermentable conditions, *psd1Δpsd2Δ* and *cho1Δ*

deletion mutant strains are strictly auxotrophic of ethanolamine because formation of endogenous Etn-P by Dpl1 is not sufficient to synthesize the required amounts of PE. In *psd1Δ* strains Psd2 is not able to provide enough PE for proper cellular growth and PE production by the ethanolamine-branch of the Kennedy pathway becomes essential (Birner et al., 2001).

In addition, PE is not only required for cellular growth but also for mitochondrial function. Deletions of *PSS1* or *PSD1* cause a decreased level of PE in mitochondria. Beside the limited PE formation under these conditions, transport of PE to mitochondrial membranes becomes growth limiting. Furthermore, *psd1Δ* mutant strains display a significant reduction of cellular and mitochondrial PE which in turn causes a *petite* phenotype characterized by a loss of respiratory capacity (Birner et al., 2001). Recently, it was discovered that lack of PE in mitochondria also results in reduced cytochrome c oxidase activity leading to a decrease of the inner membrane potential. Thus, the import of preproteins is inhibited. Moreover, depletion of PE favors the formation of larger supercomplexes (megacomplexes) between the cytochrome *bc₁* complex and the cytochrome c oxidase (Böttinger et al., 2012).

PE also serves as a precursor for GPI-anchored proteins by providing the ethanolamine phosphate bridge which links the C-terminal amino acid of GPI-anchored proteins to glycosylphosphatidylinositol. In addition, a certain level of PE in the inner mitochondrial membrane together with the prohibitin complex may be required for the attachment of mtDNA nucleoids (Nebauer et al., 2004).

1.1.2.4.3 Phosphatidylcholine (PC)

In yeast, PC is synthesized either through methylation of PE or *via* the CDP-choline branch of the Kennedy pathway (Figure 5). Yeast harbours two ER located phosphatidylethanolamine

methyltransferases which use S-adenosyl methionine (SAM) as methyl donor. Pem1/Cho2 methylates PE to yield phosphatidylmonoethanolamine, whereas Pem2/Opi3 catalyzes the second and third methylation step leading to phosphatidylcholine. Moreover, Pem2 is able to replace Pem1 to some extent, and mono- and dimethylated PE appear to be a sufficient alternative to PC in yeast. Thus, mutations in *PEM1* and *PEM2* do not render cells auxotrophic for choline (Nebauer et al., 2004). However, the Kennedy pathway is not only active upon presence of exogenous supplied choline but also functions continuously to recycle the degradation products of PC. The enzymes involved in this branch of the pathway are choline kinase (Cki1), which is able to phosphorylate choline as well as ethanolamine, cholinephosphate cytidyltransferase (Pct1/Cct1) and CDP-choline:1,2-diacylglycerol cholinephosphotransferase (Cpt1) (Daum et al., 1998).

1.2 Mitochondria

1.2.1 Phospholipids of mitochondria

Mitochondria synthesize several phospholipids autonomously including phosphatidic acid (PA), CDP-diacylglycerol (CDP-DAG), phosphatidylglycerol (PG), cardiolipin (CL) and phosphatidylethanolamine (PE). In contrast, phosphatidylserine (PS), phosphatidylcholine (PC) and phosphatidylinositol (PI) are synthesized in other organelles and thus have to be imported to mitochondria (Gebert et al., 2011).

The mitochondrial phospholipid composition varies among different cells and under different growth conditions. Nevertheless, the relative abundance of phospholipids remains within a narrow range. PC and PE are the most abundant phospholipids and comprise approximately 40% and 30% of total mitochondrial phospholipids, respectively. CL and PI

account for about 10-15% each whereas PA and PS comprise approximately 5% of total mitochondrial phospholipids (Zinser and Daum, 1995).

The lipids CDP-DAG, phosphatidylglycerol phosphate (PGP) and phosphatidylglycerol (PG) are important intermediates for the synthesis of abundant phospholipid species but do not accumulate in mitochondria under normal growth conditions. The non-bilayer forming lipids PE and CL are conical shaped with a smaller hydrophilic head group diameter and a relatively larger hydrophobic domain diameter, which allows the formation of hexagonal phases. Their tendency to form hexagonal phases creates tension in membranes which is essential for various mitochondrial processes like membrane fusion or the movement of proteins or solutes across the membrane. The unique dimeric phospholipid structure of CL affects the stability and activity of various metabolic carriers, such as ATP/ADP carrier and membrane protein complexes, as well as the respiratory chain complexes III and IV (Osman et al., 2011).

The phospholipids PC, PS and PI are primarily synthesized in the ER and imported into mitochondria as end products or precursors for other lipids. Transport of phospholipids between membranes of the ER and mitochondria, occurs at specialized fractions of the ER that are tightly associated with mitochondria, the so-called mitochondria associated membrane (MAM) fraction (Osman et al., 2011). PC, PE, PI and PS are the major phospholipids of these MAM fractions, which harbor differently accumulated phospholipid synthesizing enzymes (Gaigg et al., 1995).

Studies regarding the translocation of PS and PE between the outer and the inner mitochondrial membrane revealed that the PS transport to mitochondria is regulated by ubiquitination. A genetic screen in yeast for mutants affecting PS import into mitochondria led to the identification of the F-box protein Met30, an ubiquitin ligase (Osman et al., 2011;

Schumacher et al., 2002). Ubiquitination by Met30 results in inactivation of the transcription factor Met4, which in turn leads to an increased transport of PS from MAMs to mitochondria.

In addition, a protein complex, which functions as molecular tether between ER and mitochondria, was identified (Kornmann et al., 2009). This tethering complex consists of various proteins, namely the glycosylated ER membrane protein Mmm1, the two outer membrane proteins Mdm10 and Mdm34, respectively, and the protein Mdm12, which is associated with the outer mitochondrial membrane and an essential component for the interaction of ER and mitochondria. Cells lacking individual subunits of this ERMES (ER-mitochondrial encounter structure) complex display reduced levels of mitochondrial PE and CL. Thus, it is assumed that the ERMES complex is required for the exchange of phospholipids at ER-mitochondria contact sites (Osman et al., 2011; Schumann et al., 2002).

1.2.2 General and structural aspects of mitochondria

Mitochondria occupy up to 25% of the cytoplasmic volume and are essential for numerous cell processes, including the ATP production *via* the citric acid cycle during anaerobic metabolism (Lodish et al., 2007). These organelles have an outer and an inner membrane with folded cristae that give rise to two aqueous compartments, namely the intermembrane space and the matrix (Figure 7) (Chacinska et al., 2009). The two membranes that enclose a mitochondrion differ in composition and function. The outer membrane, composed of approximately 80% lipids and 20% proteins, contains pore proteins, which render the membrane permeable to molecules with molecular weights as high as 10000 Da (Zinser and Daum, 1995; Lodish et al., 2007). Investigation of the mitochondrial morphology by EM tomography showed that the inner membrane is in close proximity to the outer membrane

and connected to the cristae by cristae junctions of different length. Moreover, cristae, which are polymorphic and have an extensively tubular nature, can vary in their structure. Some cristae are swollen cisterns or sacs, with narrow, usually multiple tubular connections to the peripheral surface of the inner membrane and to each other, whereas other cristae are flattened with fewer interconnections to each other (Frey and Mannella, 2000).

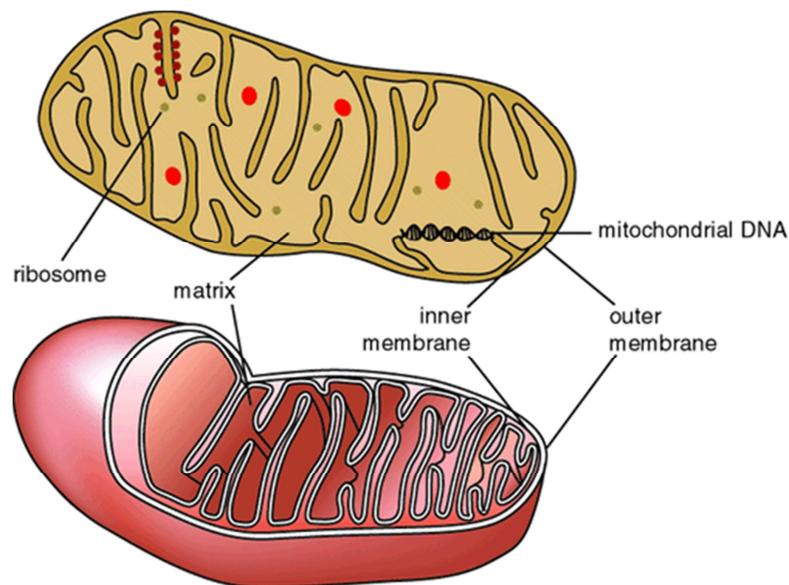


Figure 7: Structure of mitochondria. The outer membrane and the inner membrane subdivide the mitochondrion into two aqueous compartments, the intermembrane space and the matrix.

To fulfil their essential role in ATP synthesis, ion homeostasis, cell fate determination, lipid metabolisms and apoptosis, mitochondria are able to regulate and balance their number, shape and locations in different eukaryotic cell types during cell growth (Cervený et al., 2001). The budding yeast cell contains a network of mitochondrial tubules that are located near the plasma membrane and are distributed evenly in the peripheral cytoplasm. Maintenance of this tubular network requires interactions between the mitochondrial compartment and the cytoskeletal structure, which is mediated by two mitochondrial outer membrane proteins Mmm1 (mitochondrial morphology maintenance protein) and Mdm10 (mitochondrial distribution and morphology protein). In addition, two other proteins,

namely the dynamic-related GTPase Mgm1 (mitochondrial genome maintenance protein), located to the outer mitochondrial membrane, and the transmembrane GTPase Fzo1 (fuzzy onion protein) are also involved in the regulation of mitochondrial morphology. Fzo1 is required for mitochondrial fusion (Otsuga et al., 1998), whereas two other proteins are essential for organelle fission, namely the dynamic-related GTPase, Dnm1, and Net2, which binds to Dnm1 and works with the GTPase to mediate mitochondrial fission (Cervený et al., 2001).

1.2.3 The mitochondrial protein import machinery

1.2.3.1 Transport to mitochondria: targeting sequence and cytosolic chaperons

Although mitochondria have their own genome, the majority of proteins required for mitochondrial processes are encoded by nuclear genes. These proteins have to be imported into mitochondria by two distinct protein transport systems, one in the outer membrane and the other in the inner membrane (Figure 8).

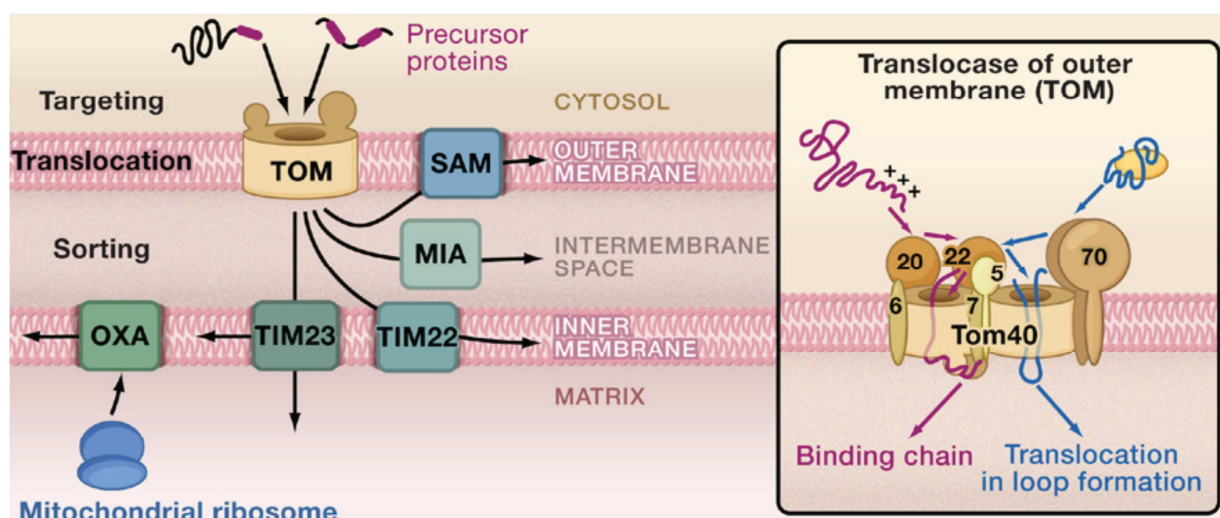


Figure 8: The mitochondrial protein import machinery (Chacinska et al., 2009)

A protein, which is destined for mitochondrial import, is normally synthesized with a transient N-terminal extension that functions as targeting signal. For proteins imported into

the matrix, this signal is a sequence of 20-30 amino acid residues, which is capable of folding into a positively charged amphiphilic helix and is removed by mitochondrial processing peptidase (Chacinska et al., 2009; Schatz, 1996).

Proteins imported into other mitochondrial subcompartments usually harbour an additional signal downstream from the mitochondrial targeting signal. This signal guides the protein to the outer membrane, the intermembrane space, or the inner membrane (Schatz, 1996). In case of a hydrophobic signal, it remains part of the mature protein and functions as membrane anchor, tethering the protein to the membrane. For several intermembrane space proteins the signal is cleaved by the inner membrane peptidase (IMP) on the outer surface of the inner membrane, and thus the mature protein is released into the intermembrane space. Protein targeted to the outer mitochondrial membrane comprises various targeting signals, located either at the N-terminal or C-terminal region of the precursor. Mitochondrial outer membrane proteins of the β -barrel type, for example, contain an internal TOM signal for the initial recognition by mitochondria, followed by a β -signal in their carboxy-terminal region (Chacinska et al., 2009).

Apart from mitochondrial targeting sequences, several molecular chaperons located in the cytoplasm mediate the transport of newly synthesised precursors to mitochondria. Chaperons, which belong to the 70 kDa heat-shock protein (hsp70) family, bind directly to the newly synthesized precursors and prevent their aggregation or irreversible misfolding. In contrast, the cytosolic chaperon MSF (mitochondrial import stimulating factor) specifically binds matrix targeting signals. Hsp70 and MSF are both ATPases whose activity is greatly stimulated by binding of non-native proteins (Schatz 1996).

1.2.3.2 The TOM complex

Mitochondrial precursor proteins are imported *via* the general entry gate, the translocase of the outer membrane (TOM complex). The TOM complex is composed of seven different subunits including the β -barrel subunit, Tom40, which forms the translocation pore, the central receptor Tom22, which inherits the receptor function and supports the oligomeric organisation of the TOM complex, and the peripheral receptors, Tom20 and Tom70, which are involved in the initial recognition of precursors. Moreover, the TOM complex comprises three small Tom proteins Tom5, Tom6 and Tom7, which regulate TOM assembly and stability (Gebert et al., 2011).

Upon protein biosynthesis, the newly synthesized precursors are bound by molecular chaperons to keep them in an unfolded state so that they can be imported into mitochondria. The N-terminal targeting sequence is recognized by import receptors Tom20 and Tom70, which subsequently transfer the precursor proteins to the general import pore Tom40. In the case of precursors destined for the mitochondrial matrix, transfer through the outer membrane occurs simultaneously with transfer through an inner membrane channel composed of Tim23 and Tim17, two proteins of the TIM (translocase of the inner membrane) complex. However, proteins that reside in the outer mitochondrial membrane are incorporated into the outer membrane by interacting with the general import pore, Tom40, and subsequently with the sorting and assembly machinery (SAM) complex (Lodish et al., 2007).

1.2.3.3 The TIM complex

Upon import through the TOM complex, precursors possessing an N-terminal targeting sequence (presequence) are handed over to the inner membrane embedded presequence

translocase, the TIM23 complex. In general, import of proteins *via* the TIM complex does not only require a motor (PAM) that drives the translocation with ATP as energy source, but also a membrane potential across the inner mitochondrial membrane (Schatz, 1996).

The TIM23 complex is composed of three essential proteins: Tim17, the channel-forming protein Tim23, and Tim50, which exposes a large domain to the intermembrane space. Tim17 is involved in recruiting the PAM complex and lateral sorting of precursors whereas Tim50 functions as receptor for incoming precursor proteins and is also involved in transient cooperation with the TOM complex (Gebert et al., 2011).

Precursors of mitochondrial carrier proteins contain uncleavable internal targeting information and require the TIM22 complex for insertion into the inner mitochondrial membrane (Bauer et al., 2000).

1.3 Phosphatidylserine decarboxylase 1 in yeast

1.3.1 General aspects of phosphatidylserine decarboxylases

One of the most abundant phospholipids of yeast membranes is PE which is mainly synthesized by phosphatidylserine decarboxylase 1 (Psd1). Psd1 belongs to type I decarboxylases and accounts for approximately 80% of cellular PSD activity. The other 20% are contributed by Psd2, a type II PSD which is localized to a Golgi/vacuole compartment. Phosphatidylserine decarboxylases are not only found in yeast, but also in other organisms, such as bacteria, fungi, plants and mammals.

Phosphatidylserine decarboxylases are membrane bound proteins and contain two non-identical subunits, which are derived from a single proenzyme. Phosphatidylserine

decarboxylases belong to a small family of decarboxylases, exhibiting a special pyruvoyl prosthetic group, required for enzymatic activity (Schuiki and Daum, 2009).

1.3.2 Characteristic sequence motifs of phosphatidylserine decarboxylase 1

PSDs display certain characteristic motifs and targeting sequences, which are essential for sorting, processing and substrate recognition. So far, various primary structures of PSDs in the range of 263 (*B. subtilis*) to 1138 amino acids (Psd2 from *S. cerevisiae*) corresponding to molecular masses of 29.7-130 kDa were identified (Schuiki and Daum, 2009). Psd1 comprises a length of 500 amino acids with a molecular mass of 56.6 kDa (Clancey et al., 1993). In contrast, the *PSD2* gene from *S. cerevisiae* encodes a protein with a length of 1138 amino acids and a predicted molecular mass of 130 kDa (Trotter et al., 1995). The deduced protein sequences of *PSD1* and *PSD2* genes show only 12.6% identity to each other (Schuiki and Daum, 2009). However, Psd1 from *S. cerevisiae* shares 44% and 35% identity with Psds from CHO cells and *E. coli*, respectively (Clancey et al., 1993).

PSDs from various sources feature a characteristic GST motif near the C-terminus of the proenzyme. During post-translational processing, autocatalytic cleavage at this special motif gives rise to the mature and active enzyme, comprising an α - and a β -subunit (Schuiki and Daum, 2009). The GST motif of type I phosphatidylserine decarboxylases is usually formed by a highly conserved LGST sequence, which is found at amino acids 461-464 in Psd1 from yeast (Trotter et al., 1993). Type II phosphatidylserine decarboxylases typically comprise a GGST motif (Trotter et al., 1995). Beside the conserved GST motifs at the C-terminus of the proenzyme, phosphatidylserine decarboxylases also exhibit special domains at the N-terminus. Type I phosphatidylserine decarboxylases contain domains for protein targeting to the inner mitochondrial membrane and the inner membrane space, whereas type II

enzymes harbour putative targeting sequences for the endomembrane system (Figure 9) (Schuiki and Daum 2009).

A: Type I PSD



B: Type II PSD



Figure 9: Structural organization of eukaryotic type I and type II PSDs. (A) Type I PSDs contain a mitochondrial targeting sequence (MT), an intermembrane space sorting sequence (IM), an α - and a β -subunit, and a typical cleavage site LGST. (B) Type II PSDs contain putative endomembrane system targeting sequences (EMS), a C2 homology domain (C2), an α - and a β -subunit, and a typical cleavage site GGST.

Another consensus motif detected in PSDs is the peptide FFXLKXXXKXR, found in CHO cells (amino acids 351-362) and in yeast Psd1 (amino acids 475-486), but not in *E. coli*. This motif is located to the α -subunit in close proximity to the catalytic carbonyl group and is thought to facilitate the specific interaction of the enzyme with the substrate PS. Moreover, a sequence similar to the phosphatidylserine binding peptide motif in Psd1 has been detected in yeast Psd2. This substrate recognition site resides in the C2 homology domain, which functions as Ca^{2+} and phospholipid binding site (Igarashi et al., 1995).

Recently, it was shown that Psd1 from the yeast *Saccharomyces cerevisiae* contain a hydrophobic domain within its β -subunit (amino acids 80-100) tethering the enzyme to the inner mitochondrial membrane. The C-terminus faces the intermembrane space and anchors the α -subunit to this compartment (Figure 10) (Horvath et al., 2012).

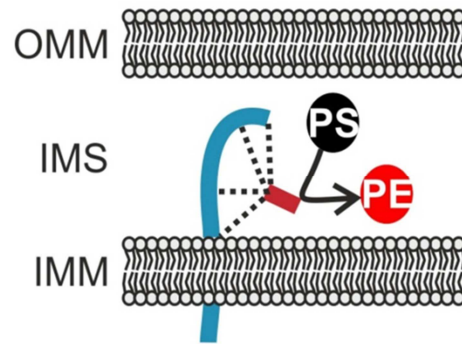


Figure 10: Model of phosphatidylserine decarboxylase 1. Psd1 is tethered to the inner mitochondrial membrane by its β -subunit (red: α -subunit; blue: β -subunit).

1.3.3 Biogenesis and processing of phosphatidylserine decarboxylase 1

Phosphatidylserine decarboxylase 1 is encoded by the nuclear genome and synthesized on cytosolic ribosomes. It has to be imported into mitochondria where it catalyses the formation of PE from PS. Thus, Psd1 displays an N-terminal mitochondrial targeting sequence followed by an inner mitochondrial membrane sorting signal. The N-terminal sequence is rich in positively charged residues and poor in acidic amino acids which is a typical feature of mitochondrial targeting sequences (Schuiki and Daum, 2009).

The first step in the mitochondrial import process of proteins, which are synthesized on cytosolic ribosomes, is the translocation across the outer mitochondrial membrane. This step is mediated by the translocase of the outer membrane import machinery (TOM complex). The TOM complex consists of the translocation channel Tom40, the peripheral receptors Tom20 and Tom70, the central organizer Tom22 and other low molecular-weight TOM subunits. In general, the Tom20 receptor recognizes precursors with N-terminal targeting signals, whereas Tom70 interacts with hydrophobic precursor proteins containing internal targeting sequences (Baker et al., 2007). Studies with mitochondria lacking either Tom22 or one of the two peripheral receptors showed that Tom70 and Tom22 are the main

receptors for the import of the Psd1 precursor into mitochondria (Horvath et al., 2012). Upon import three forms of Psd1 could be detected: intermediate 1 and 2 and the mature Psd1 β -subunit. The cleavage of the Psd1 precursor into an α - and a β -subunit is a crucial step in the formation of the active centre of the enzyme and occurs independently from the import process mediated by Tom70. Moreover, mislocalization of Psd1 to the matrix site of the inner membrane did not impair its self-cleavage, indicating that proper maturation and targeting of Psd1 within mitochondria is not essential for separation of the two subunits.

The assembly of Psd1 into the inner mitochondrial membrane requires an energized inner mitochondrial membrane translocation system (TIM complex) (Horvath et al., 2012). The sorting mechanism of the Psd1 precursor into the inner mitochondrial membrane is not known but it has been demonstrated that an internal hydrophobic region within the Psd1 sequence (80 to 100 amino acids) functions as membrane anchor tethering Psd1 to the inner mitochondrial membrane *via* its β -subunit.

Recently, two matrix-localized processing peptidases MPP and Oct1, which are involved in removing the targeting signals from the Psd1 precursor, could be identified (Figure 11) (Horvath et al., 2012). MPP usually cleaves the mitochondrial sequence and subsequently Oct1 removes a small octapeptide. In general, the processing step catalysed by Oct1 is considered to stabilize the N-terminus of the mature Psd1.

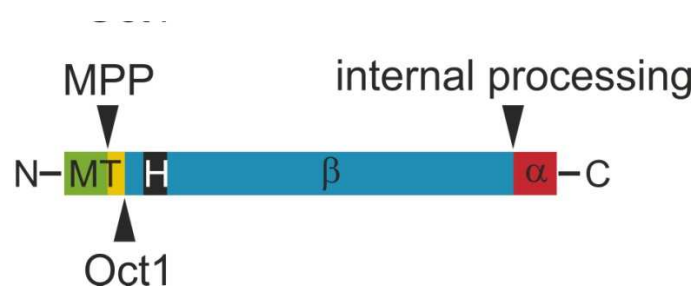


Figure 11: Psd1 processing. Internal processing leads to the active and mature enzyme with a soluble α -subunit and a membrane bound β -subunit.

Processing of type II phosphatidylserine decarboxylases has been proposed to occur similar to type I enzymes. However, it has shown that neither the putative Golgi retention/localization signal nor the C2 homology domain of the yeast Psd2 is involved in proper localization of the polypeptide (Kitamura et al., 2002).

1.3.4 Enzymatic properties of phosphatidylserine decarboxylase 1

1.1.3.4.1 Enzymology of phosphatidylserine decarboxylases

The GS amino acid residues of the typical motif found in all phosphatidylserine decarboxylases is not only the site of autocatalytic cleavage into an α - and a β -subunit, but also plays an essential role in the formation of the catalytic pyruvoyl group of the mature enzyme. Since unprocessed phosphatidylserine decarboxylases are inactive, the GS residues can be regarded as essential for active α -subunits and thus for enzymatic activity (Nebauer et al., 2007).

The mechanism of the autocatalytic event comprises serinolysis of the peptide bond between the glycine and the serine residue of the highly conserved LGST motif resulting in the formation of an ester bond between the two amino acids. Afterwards, an α,β elimination reaction leads to the release of the β -chain, leaving a dehydroalanine at the amino terminus of the α -subunit. Finally, addition of water across the double bond gives rise to the α -hydroxy alanyl residue which subsequently forms the pyruvoyl moiety upon elimination of ammonia (Figure 12) (Voelker, 1997).

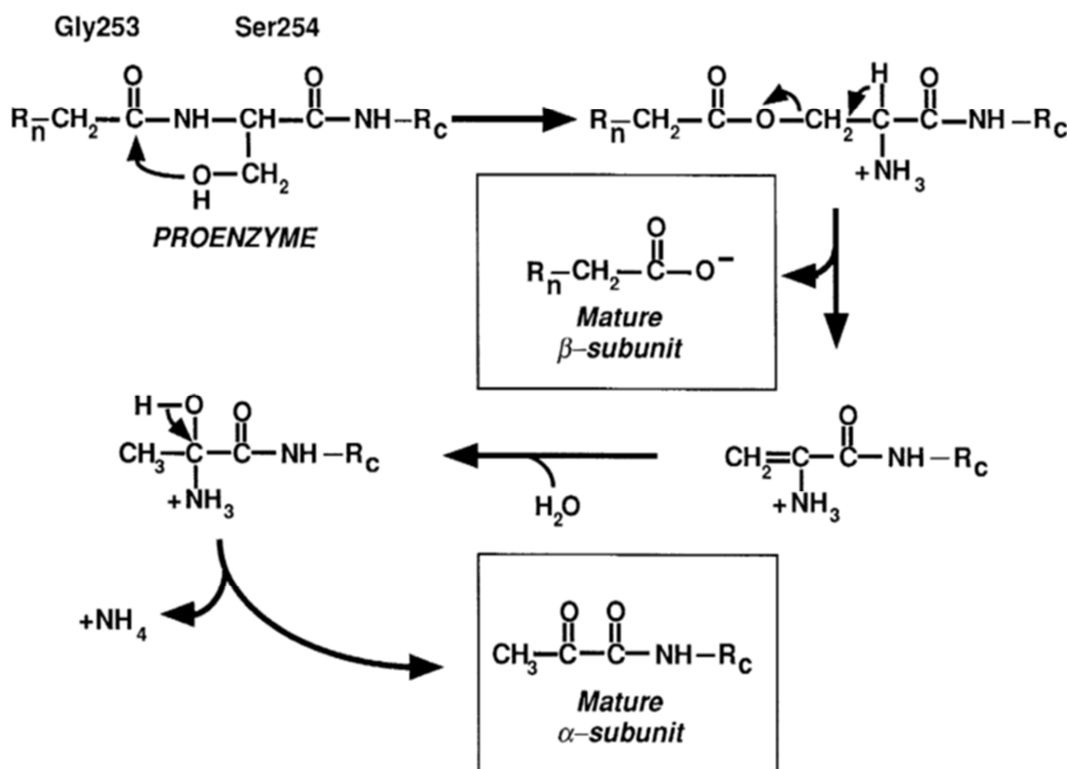


Figure 12: Mechanism of pyruvoyl prosthetic group formation in bacterial PSD (Voelker et al., 1997)

The proposed reaction scheme for *E. coli* phosphatidylserine decarboxylase (Figure 13) involves decarboxylation of PS *via* the formation of a Schiff's base between the α -carbonyl carbon of the covalently bound pyruvoyl prosthetic group and the primary amine of serine from the substrate. Electron rearrangement supports the decarboxylation and formation of an azomethin intermediate, followed by protonation, which generates the product, PE, in Schiff's base linkage with the enzyme. Finally, addition of water across the Schiff's base regenerates the pyruvoyl prosthetic group and releases PE from the active site of the enzyme (Nebauer et al., 2007; Voelker, 1997).

In addition, it has been suggested that the enzymatic reaction of Psd2 also occurs through Schiff's base formation of the active site of the enzyme. However, the C2 domain is rather required for the recruitment of PS from donor membranes than for catalytic activity (Kitamura et al., 2002).

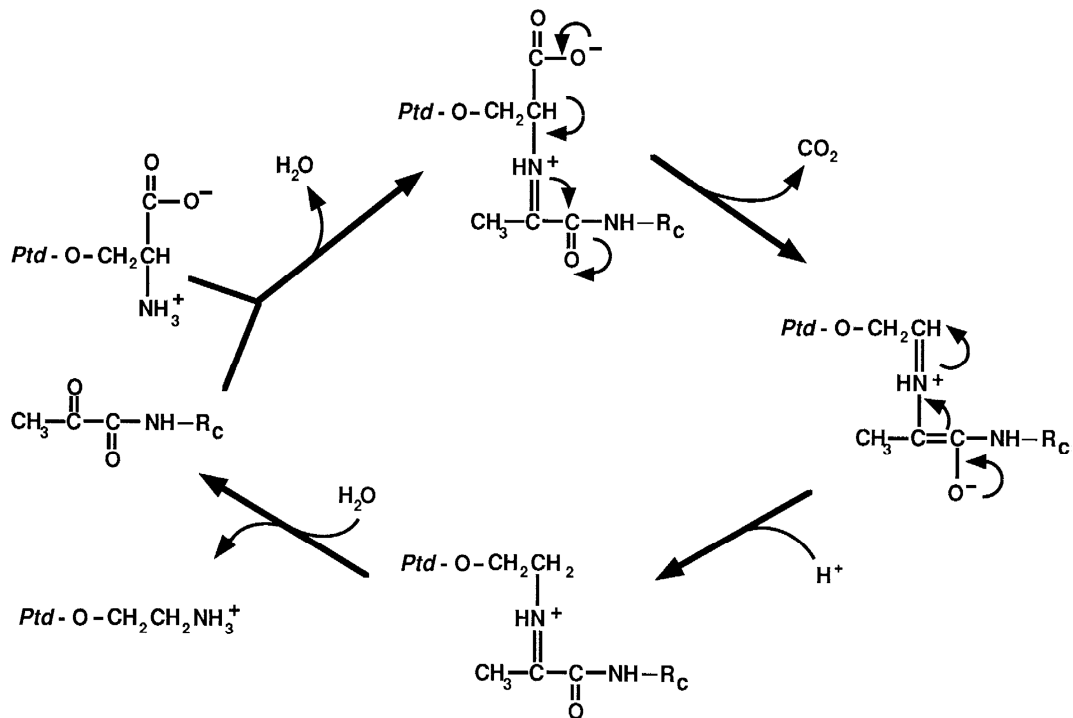


Figure 13: Proposed reaction scheme for decarboxylation of PS (Voelker, 1997)

1.1.3.4.2 Regulation of phosphatidylserine decarboxylase activity

In the promoter region of the *PSD1* gene three sequences homologue to the consensus sequence of the inositol choline response element UAS_{INO} were found. Thus, the expression of the *PSD1* gene is regulated in the same way as the expression of other coregulated genes of the CDP-DAG pathway, like *CHO1* (PS synthase) or *CHO2/PEM1* (PE methyltransferase). In the absence of inositol, heterodimers of the transcriptional regulators Ino2 and Ino4 bind to the UAS_{INO} to activate transcription, whereas addition of inositol to the growth media of growing cells causes translocation of Opi1 to the nucleus, where it represses transcription of the respective gene. However, Psd2 is not subject to regulation by inositol (Griac, 1997; Jesch et al., 2005).

2 Aims of the thesis

The aim of this master thesis was molecular characterization of phosphatidylserine decarboxylase 1 from yeast. To get more information about specific regions within the sequence of Psd1 including two predicted transmembrane domains (IM1 and IM2) and a potential substrate recognition site, a series of Psd1 variants lacking SRS, IM2 or both transmembrane domains were generated. Characterization of the respective mutants comprises localization experiments, enzymatic analysis with radiolabeled substrates and phospholipid profiling.

Major points of the master thesis include:

- Cloning and verification of Psd1 mutants, lacking IM2, IM1+2 and SRS
- Isolation of mitochondria from strains expressing Psd1 variants
- Quality control of isolated subcellular fractions
- Localization studies by treatment of intact, hypo-osmotically swollen and lysed mitochondria with proteinase K
- Investigation of the Psd1 membrane association with carbonate extraction
- Phospholipid profiling of homogenate and mitochondria
- Determination of Psd1 activity in wild type and Psd1 mutant strains using radioactive labeled substrate

3 Materials and Methods

Chemicals used throughout this study were purchased by following companies: Sigma-Aldrich, Roth or Merck. Restriction enzymes and Phusion High-Fidelity DNA polymerase were obtained from Fermentas, whereas Go Taq DNA polymerase was obtained from Promega.

3.1 Strains and culture conditions

3.1.1 *E. coli* strains and culture conditions

E. coli strains and plasmids used in this study are listed in Table 1- 2.

Table 1: Plasmids and their genotype

Strains and plasmids	Relevant genotype	Source of reference
pSH4	pYES2 + <i>PSD1ΔIM1</i>	Horvath et al., 2012
pSTH1	pYES2 + <i>PSD1ΔIM2</i>	This study
pSTH2	pYES2 + <i>PSD1ΔIM1+2</i>	This study
pSTH3	pYES2 + <i>PSD1ΔSRS</i>	This study

Table 2: *E. coli* strains and their genotype

Strains and plasmids	Relevant genotype	Source of reference
SH4	<i>E. coli</i> TOP 10 F ⁻ <i>mcrA</i> Δ(<i>mrr-hsdRMS-mcrBC</i>) φ80 <i>lacZ</i> ΔM15 Δ <i>lacX74</i> <i>deoR</i> <i>nupG</i> <i>recA1</i> <i>araD139</i> Δ(<i>ara-leu</i>)7697 <i>galU</i> <i>galK</i> <i>rpsL</i> (Str ^R) <i>endA1</i> λ + pSH4	Horvath et al., 2012
STH1	<i>E. coli</i> TOP 10 F ⁻ <i>mcrA</i> Δ(<i>mrr-hsdRMS-mcrBC</i>) φ80 <i>lacZ</i> ΔM15 Δ <i>lacX74</i> <i>deoR</i> <i>nupG</i> <i>recA1</i> <i>araD139</i> Δ(<i>ara-leu</i>)7697 <i>galU</i> <i>galK</i> <i>rpsL</i> (Str ^R) <i>endA1</i> λ + pSTH1	This study
STH2	<i>E. coli</i> TOP 10 F ⁻ <i>mcrA</i> Δ(<i>mrr-hsdRMS-mcrBC</i>) φ80 <i>lacZ</i> ΔM15 Δ <i>lacX74</i> <i>deoR</i> <i>nupG</i> <i>recA1</i> <i>araD139</i> Δ(<i>ara-leu</i>)7697 <i>galU</i> <i>galK</i> <i>rpsL</i> (Str ^R) <i>endA1</i> λ + pSTH2	This study
STH3	<i>E. coli</i> TOP 10 F ⁻ <i>mcrA</i> Δ(<i>mrr-hsdRMS-mcrBC</i>) φ80 <i>lacZ</i> ΔM15 Δ <i>lacX74</i> <i>deoR</i> <i>nupG</i> <i>recA1</i> <i>araD139</i> Δ(<i>ara-leu</i>)7697 <i>galU</i> <i>galK</i> <i>rpsL</i> (Str ^R) <i>endA1</i> λ + pSTH3	This study

E. coli strains were grown over night on LBA media at 37°C and 120 rpm. Selective LB plates supplemented with ampicillin were used for strain construction and contained the following components listed in Table 3 and 2% agar.

Table 3: Composition of LB media and LB plates

Component	Concentration
Yeast Extract	5 g/L
NaCl	5 g/L
Tryptone	10 g/L
100 µg/mL ampicillin was added for <i>E. coli</i> strains containing an ampicillin selective marker	

3.1.2. *Saccharomyces cerevisiae* strains and culture conditions

Saccharomyces cerevisiae strains used in this study are listed in Table 4.

Table 4: Strains and their genotype

Strains and plasmids	Relevant genotype	Source of reference
wild type	BY4741 MATa <i>his3Δ1 leu2Δ0 met15Δ0 ura3Δ0</i>	Euroscarf collection (Frankfurt, Germany)
psd1Δ	BY4741 MATa <i>his3Δ1 leu2Δ0 met15Δ0 ura3Δ0 psd1Δ::KanMx4</i>	Euroscarf collection (Frankfurt, Germany)
WT + pYES2	BY4741 MATa <i>his3Δ1 leu2Δ0 met15Δ0 ura3Δ0</i> + pYES2	Horvath et al., 2012
psd1Δ + pYES2	BY4741 MATa <i>his3Δ1 leu2Δ0 met15Δ0 ura3Δ0 psd1Δ::KanMx4</i> + pYES2	
Psd1HA	BY4741 MATa <i>his3Δ1 leu2Δ0 met15Δ0 ura3Δ0 psd1Δ::KanMx4</i> + pYES2- <i>PSD1HA</i>	
Psd1S463A	BY4741 MATa <i>his3Δ1 leu2Δ0 met15Δ0 ura3Δ0 psd1Δ::KanMx4</i> + pYES2- <i>PSD1S463A</i>	
Psd1ΔIM	BY4741 MATa <i>his3Δ1 leu2Δ0 met15Δ0 ura3Δ0 psd1Δ::KanMx4</i> + pYES2- <i>PSD1ΔIM</i>	
YSTH1	BY4741 MATa <i>his3Δ1 leu2Δ0 met15Δ0 ura3Δ0 psd1Δ::KanMx4</i> + pSTH1	This study
YSTH2	BY4741 MATa <i>his3Δ1 leu2Δ0 met15Δ0 ura3Δ0 psd1Δ::KanMx4</i> + pSTH2	This study
YSTH3	BY4741 MATa <i>his3Δ1 leu2Δ0 met15Δ0 ura3Δ0 psd1Δ::KanMx4</i> + pSTH3	This study

For precultures, strains were grown on YPD, whereas strains containing high expression GAL plasmids were grown on -ura Glucose under aerobic conditions to the stationary phase at

30°C and 120 rpm (Table 5-6). For induction of Psd1 expression –ura selective media containing galactose as a carbon source was used. In the case of poorly growing mutant strains 2% glucose was added to the main culture (Table 7). Selective plates lacking the appropriate amino acid were used for strain construction and contained the following components listed in Table 5-7 and 2% agar.

Table 5: Composition of YPD media

Media	Component	Concentration
YPD	Yeast Extract	10 g/L
	Peptone	20 g/L
	Glucose	20 g/L

Table 6: Composition of -ura Glucose media

Media	Component	Concentration
-ura Glucose	Glucose	20 g/L
	Yeast Nitrogen Base	6.7 g/L
	-ura amino acid stock	0.63 g/L

Table 7: Composition of -ura Galactose media

Media	Component	Concentration
-ura Galactose	Galactose	20 g/L
	Yeast Nitrogen Base	6.7 g/L
	-ura amino acid stock	0.63 g/L

3.2 Plasmids and strain construction

3.2.1 Overlap-extension PCR

In order to generate yeast strains expressing *PSD1ΔIM2*, *PSD1ΔIM1+2* and *PSD1ΔSRS* overlap-extensions PCR was used (Figure 14-16). Templates and primers used for overlap-extension PCR are listed in Table 8-9.

Table 8: Plasmids used for overlap-extension PCR

Cassette	Template Plasmid
<i>PSD1ΔIM2</i>	pYIS5*
<i>PSD1ΔIM1+2</i>	pSH4
<i>PSD1ΔSRS</i>	pYIS5*

(*provided by Irmgard Schuiki)

Table 9: Primers used for overlap-extension PCR

Cassette	Primer	Sequence (5' to 3')
<i>PSD1ΔIM2</i> <i>PSD1ΔIM1+2</i>	STH1 rev. (‘inner’ primer 1)	TTTACTTGGCCCCATATTTTGATTTTCTTGCCTTCTC CCTTTTTGCC
	STH2 for. (‘inner’ primer 2)	GACAAGAAAAATCAAATATGGGGCCAAGTAAATTC TCTTACGTTACCCA
	SH1 rev. (‘outer’ primer 2)	TTGCGGCCGCAATCAAGCGTAGTCTGGGACGTCGTAT GGGTATTTTAAATCATTCTTTCCAATTATGCC
	PSD1_Bam_HI_OE for. (‘outer’ primer 1)	CGCGGATCCGCGAGCAGATCGCTCAAATCCTTCTTG GTCGTTAT
<i>PSD1ΔSRS</i>	STH3 rev. (‘inner’ primer 1)	GCCTAATTTCTGTCCCATTTTCAGTGGGAGCTTCAAAA CAAAGTACAACAG
	STH4 for. (‘inner’ primer 2)	TGAAGCTCCCACTGAAATGGGACAGAAATTAGGCAT AATTGGAAAGAATG
	SH1 rev. (‘outer’ primer 2)	TTGCGGCCGCAATCAAGCGTAGTCTGGGACGTCGTAT GGGTATTTTAAATCATTCTTTCCAATTATGCC
	PSD1_Bam_HI_OE for. (‘outer’ primer 1)	CGCGGATCCGCGAGCAGATCGCTCAAATCCTTCTTG GTCGTTAT

In order to delete the transmembrane domain (IM2) and the substrate recognition site (SRS), respectively, within the *PSD1* sequence a special set of two ‘inner’ and two ‘outer’ primers was used. In two separate PCR reactions using each time a mating ‘inner’ and ‘outer’ primer, two PCR fragments (fragment I and fragment II), excluding the deletion domain, were

generated. The ‘inner’ primers were designed with extended overhang regions at their 5’-end, which permitted ligation of the resulting two fragments.

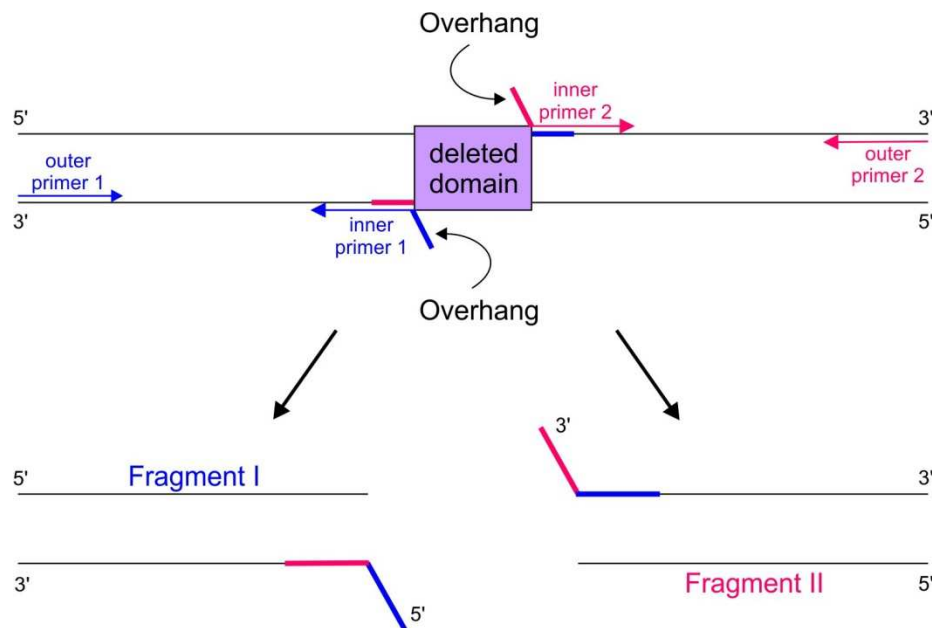


Figure 14: Generation of fragment I and fragment II

Both fragments obtained from the first PCR-step (Table 10-11) were visualized and purified by gel-electrophoresis. After separation the expected sizes of bands were examined by using a standard MassRuler™ DNA Ladder Mix (MBI Fermentas) and a DNA imager (BIORAD Gel Doc 2000). Fragments were purified with a Gel Extraction Kit according to the manufacturer's protocol (OMEGA/Nucleo Bond).

Table 10: Composition of the reaction mix used in the first step of the overlap-extension PCR

Component	Volume [μL]
Template (250 ng/ μL)	2
Primer_reverse (10 pmol/ μL)	2
Primer_forward (10 pmol/ μL)	2
2.5 mM dNTP Mix	4
5 x Phusion Buffer HF	10
Phusion HF Polymerase (2u/ μL)	0.5
Fresenius-H ₂ O	fill up to a total volume of 50 μL

Table 11: Cycle parameter of the first step of the overlap-extension PCR

Phase	Temperature [°C]	Time	Cycles
Initial denaturation	98	30 sec.	
Denaturation	98	10 sec.	15
Annealing	60	20 sec.	
Extension	72	1 min./kb	
Final Extension	72	7 min.	

In a second PCR-step (Figure 15), fragment I and fragment II were ligated, giving rise to *PSD1* mutants either lacking the transmembrane domain 2 (IM2) or the substrate recognition site (SRS). Thus, equimolar DNA amounts of both fragments were used in a PCR-mix without primers (Table 12-13).

Table 12: Composition of the reaction mix used in the second step of the overlap-extension PCR

Component	Volume [μL]
2.5 mM dNTP Mix	24
5 x Phusion Buffer HF	60
Phusion HF Polymerase (2u/μL)	3
Fresenius-H ₂ O	192
300 ng of the larger fragment (<i>PSD1ΔIM2</i> : 1080 bp; <i>PSD1ΔSRS</i> : 1400 bp)	
90 ng of the smaller fragment (<i>PSD1ΔIM2</i> : 420 bp; <i>PSD1ΔSRS</i> : 7 bp)	
The PCR-mix is divided into 6 PCR tubes each containing 50 μL of the reaction mix.	

Table 13: Cycle parameter of the second step of the overlap-extension PCR

Phase	Temperature [°C]	Time	Cycles
Initial denaturation	98	30 sec.	
Denaturation	98	10 sec.	35
Annealing	60	20 sec.	
Extension	72	1 min./kb	
Final Extension	72	7 min.	

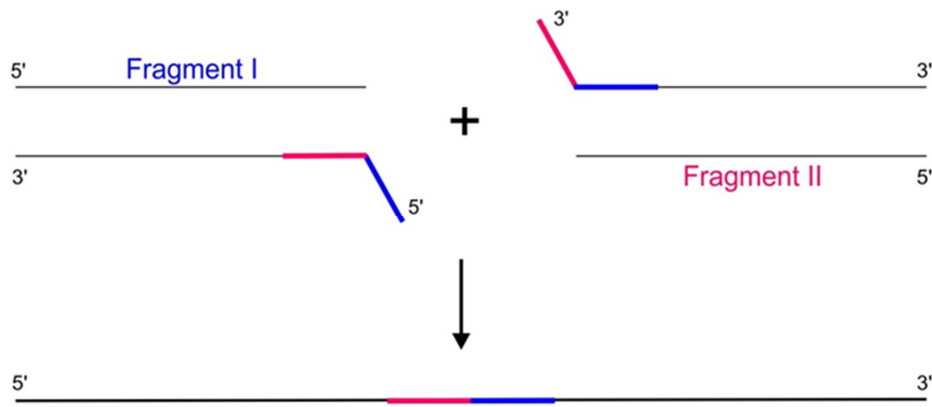


Figure 15: Ligation of fragment I and fragment II

After 35 PCR cycles 50 μL of a second PCR-mix containing polymerase and the ‘outer’ primers SH1 and PSD1_Bam_HI_OE were added to the reaction (Table 14). After amplification according to Table 15 the *PSD1* sequence without the respective domain was generated (Figure 16). Finally, the resulting PCR-products were again separated by agarose gel electrophoresis, isolated and purified by Gel Extraction Kit (OMEGA/Nucleo Bond).

Table 14: Composition of the second reaction mix used for overlap-extension PCR

Component	Volume [μL]
PSD1_Bam_HI_OE for. (10 pmol/ μL)	24
SH1 rev. (10 pmol/ μL)	24
2.5 mM dNTP Mix	24
5 x Phusion Buffer HF	60
Phusion HF Polymerase (2u/ μL)	1.8
Fresenius-H ₂ O	166.2

Table 15: Cycle parameters of the third step of overlap extension PCR

Phase	Temperature [$^{\circ}\text{C}$]	Time	Cycles
Initial denaturation	98	30 sec.	
Denaturation	98	10 sec.	25
Annealing	60	20 sec.	
Extension	72	1 min./kb	
Final Extension	72	7 min.	

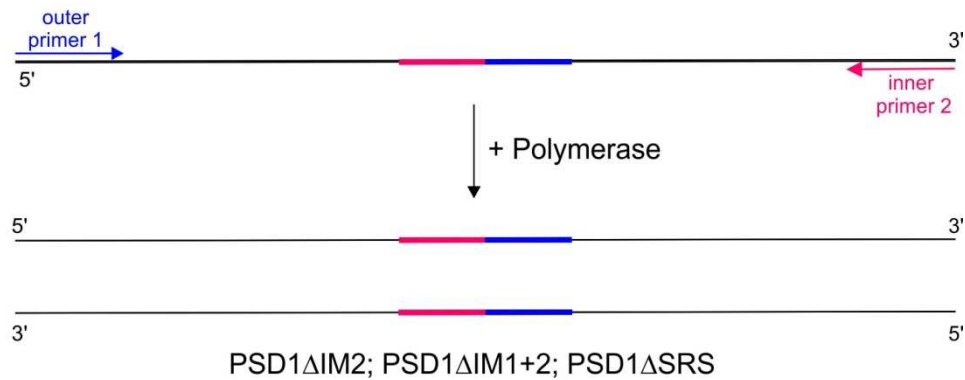


Figure 16: Amplification of the OE-PCR product

3.2.2 Ligation and transformation in *E. coli*

After generation of *PSD1ΔIM2*, *PSD1ΔIM1+2* and *PSD1ΔSRS* by overlap-extension PCR, the PCR-products were ligated into a pYES2 vector (Figure 17).

The pYES2 vector comprises a *GAL1* promoter, which permits inducible expression of genes cloned into the vector, a T7 promoter/priming site, which allows for *in vitro* transcription in the sense orientation and sequencing through the insert and a *CYC1* transcription termination signal, which permits efficient termination and stabilization of mRNA. Moreover, the pYES2 vector features a multiple cloning site with 9 unique sites, which allows insertion of a gene into the vector, an ampicillin resistance gen, which permits selection of transformants in *E. coli* and a *URA3* gene, which allows for selection of yeast transformants in uracil-deficient medium. The pYES2 vector also displays a pUC and a 2 μ origin for maintenance and high copy replication in *E. coli* and a f1 origin, which permits rescue of single-stranded DNA (Figure 17).

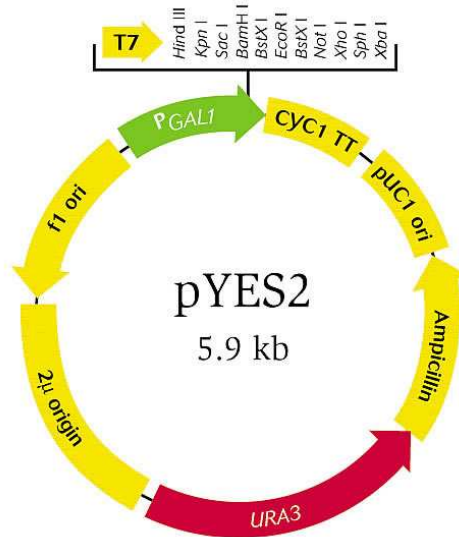


Figure 17: pYES2 vector

The pYES2 vector and the overlap extension PCR-products (*PSD1ΔIM2*, *PSD1ΔIM1+2* and *PSD1ΔSRS*) both feature restriction sites for BamHI and NotI. These restriction sites were used for insertion of *PSD1ΔIM2*, *PSD1ΔIM1+2* and *PSD1ΔSRS* into the vector. First, the pYES2 vector and the respective overlap-extension PCR-product (insert) were restricted with BamHI and NotI (Table 16) for 2 h at 37°C. After restriction, the vector and the PCR-products were subjected to agarose gel electrophoresis, isolated and purified by Gel Extraction Kit (OMEGA/Nucleo Bond).

Table 16: Reaction mix used for vector and insert restriction

Component	Volume [μL]
Vector restriction	
Bam_HI_Buffer	4
BamHI (10 u/μL)	1
NotI (10 u/μL)	3
600 ng pYES2 vector (250 ng/μL)	2.4
Fresenius-H ₂ O	29.6
insert restriction	
Bam_HI_Buffer	4
BamHI (10 u/μL)	1
NotI (10 u/μL)	3
600 ng insert	depending on the concentration
fill up to 40 μL with Fresenius-H ₂ O	

The restricted and purified pYES2 vector and respective insert (*PSD1ΔIM2*, *PSD1ΔIM1+2* or *PSD1ΔSRS*) were ligated at for 2 h at 22°C and 300 rpm (Table 17). The ligation of insert and vector was followed by inactivation of the restriction enzymes for 10 min at 65°C.

Table 17: Reaction mix used for ligation of vector and insert

Component	Volume [μL]
10 x T ₄ -DNA Ligase Buffer	3
T ₄ -DNA Ligase (1 Weiss u/μL)	1.5
50 ng pYES2 vector (5799 bp)	depending on the concentration
38.8 ng insert (1500 bp)	depending on the concentration
fill up to 30 μL with Fresenius-H ₂ O	

The deployed amount of insert was determined as follows:

$$ng (insert) = \frac{bp (insert) * ng (vector)}{bp (insert)} * 3$$

For subsequent transformation in *E. coli* 100 μL gentle thawed *E. coli* TOP10 competent cells were mixed with 20 μL of the inactivated ligation mix and incubated from 30 min on ice. After incubation for 2 min at 42°C samples were cooled down for 1 min on ice. 900 μL LB-medium was added to the samples, which were subsequently incubated for 0.5-1 h at 37°C. After transformation all cells were plated on LB-plates with ampicillin as selective markers. Negative controls were performed for all experiments.

3.2.3 TELT method: a quick method for plasmid isolation

The TELT method was used for fast plasmid isolation. *E. coli* colonies were picked from selective plates and grown over night in 5 mL LBA-media at 37°C and 120 rpm. 1.5 mL of each overnight culture was centrifuged (Heraeus FRESCO 17 centrifuge) and resulting pellets were resuspended in 440 μL TELT solution containing 10 mg/mL lysozyme (Table 18). Samples were first incubated for 10 min at room temperature, 2 min at 95°C and 10 min on ice. After centrifugation for 10 min at room temperature, proteins, chromosomal DNA and

cell fragments remained in the pellet whereas plasmid DNA was found in the supernatant. The pellet was removed and 260 μL isopropanol (RT) was added. Samples were incubated on ice for 10 min, centrifuged with maximum speed at 4°C for 10 min and washed with 70% ethanol. Finally, the pellets were resuspended in 25 μL Fresenius-H₂O.

Table 18: Composition of the TELT reagent

Component	Concentration
Tris HCl	50 mM
EDTA	62.5 mM
Lithium acetate	2.5 mM
Triton X-100	0.4 %

3.2.4 Restriction

Successful ligation of the insert cassette into pYES2 vector was verified by restriction analysis using BamHI and NotI (Table 19) for 2 h at 37°C. Restriction products were examined for the expected size of the insert by agarose-gel electrophoresis. Positive clones displaying vector and insert after restriction were sequenced and used for further studies.

Table 19: Reaction mix used for plasmid and vector restriction

Component	Volume [μL]
Bam_HI_Buffer	2
BamHI (10 u/ μL)	0.5
NotI (10 u/ μL)	1.5
Plasmid/Vector	4
Fresenius-H ₂ O	12

3.3 Plasmid transformation in the yeast *Saccharomyces cerevisiae*

3.3.2 Lithium Acetate Transformation

The verified and sequenced plasmids *PSD1 Δ IM2*, *PSD1 Δ IM1+2* and *PSD1 Δ SRS* were transformed into *psd1 Δ* yeast cells by the lithium acetate method (Gietz et al., 1992). Yeast

cells were grown overnight in 25 mL YPD media at 30°C and 120 rpm. After measuring the optical density at 600 nm (Hitachi U-1100 UV/VIS spectrometer) 25 mL of fresh media was inoculated to an OD₆₀₀ of 0.3 with the overnight culture. Cells were grown until an OD₆₀₀ of 0.8 to 1.0 and harvested by centrifugation at 4500 rpm for 5 min at room temperature (Hettich Rotina 46 R). After resuspending the pellet in 200 µL TE/LiAc, cells were incubated for 30 min on ice. For each transformation, 50 µL competent cells were transferred to a sterile Eppendorf tube and mixed with 2 µL plasmid, 5 µL HsDNA and 300 µL TE/LiAc/PEG. As negative control H₂O instead of plasmid DNA, was used. The suspension was mixed by inverting the tube several times. Cells were regenerated at 30°C for 20 min with agitation at 1100 rpm. After heat shock for 15 min at 42°C and cooling on ice, the cell suspension was plated on selective plates, where the appropriate amino acid was omitted for selection purpose (-ura Glucose). The cultures were incubated at 30°C for several days. Successful transformation of the plasmid in *psd1Δ* mutant strains was verified by colony-PCR.

Table 20: Solution used for Lithium Acetate Transformation

Solution	Reagent
10 x TE buffer	100 mM Tris 10 mM EDTA pH 7.5 (with HCl)
10 x LiAc	1 M LiAc*2 H ₂ O pH 7.5 (with diluted acetic acid)
50% PEG 4000	50% (w/v) PEG
TE/LiAc	1 x TE buffer 100 mM LiAc
TE/LiAc/PEG	1 x TE buffer 100 mM LiAc 40% PEG
hsDNA	10 mg/mL

3.3.3 Colony-PCR

Colony-PCR is a common method used for screening yeast transformants for correct insertion or deletion products. Therefore, selected colonies were picked with a sterile pipette tip from a growth plate, transferred into PCR tubes containing 25 μL sterile water and lysed for 8 min at 99°C (2720 Thermo Cycler) to ensure that proteases were inactivated. After centrifugation for 30 sec at 1300 rpm and 4°C (Hereaus FRESCO 17), 5 μL of each supernatant (DNA templates) were transferred into fresh PCR tubes containing 20 μL colony-PCR master mix (Table 21). Primers either annealing on the plasmid for verification of correct plasmid transformation or on the chromosome for background information were used. All primers and parameters for the PCR reactions are listed in Table 22-23.

Table 21: Composition of the PCR-colony master mix

Component	Volume [μL]
H ₂ O	10.7
5 x green buffer	4
2.5 mM dNTP	2
Forward Primer (25 pmol/ μL) (Table 22)	1.5
Reverse Primer (25 pmol/ μL) (Table 22)	1.5
Go Taq Polymerase (5u/ μL)	0.3

Table 22: Primers used for colony-PCR

Cassette	Primer	Sequence (5'-3')
<i>psd1Δ</i>	PSD1-A1 for. kanMX4 rev.	GGTTGTTTATGTTCCGGATGTG GTTGTTTATGTTCCGGATGTG
pYES2- <i>PSD1ΔIM2</i> pYES2- <i>PSD1ΔIM1+2</i> pYES2- <i>PSD1ΔSRS</i>	GAL1-Prom2 for. PSD1-A2 rev.	GCAGTAACCTGGCCCCAC GGAGACCTGTTTTCTTCCGC

Table 23: Cycle parameters for colony-PCR

Phase	Temperature [°C]	Time	Cycles
Initial denaturation	95	2 min.	
Denaturation	95	30 sec.	25
Annealing	53	30 sec.	
Extension	72	1 min./kb	
Final Extension	72	12 min.	

Transformants containing the plasmid and correct genomic background display DNA bands of expected size which were separated by agarose gel-electrophoresis and visualized by gel imaging using a documentary system (BIORAD Gel Doc 2000).

3.4 Organelle preparation – Isolation of mitochondria

Isolation of mitochondria was performed according the established procedure for the yeast *Saccharomyces cerevisiae* described by Zinser and Daum (1995).

3.4.1 Growth of *Saccharomyces cerevisiae* BY4741 and various mutant strains

Precultures were grown under aerobic conditions to stationary growth phase in 200 mL -ura Glucose media (Table 6) at 30°C with shaking at 120 rpm. Mitochondria were isolated from cells grown to a final OD₆₀₀ of 1.5 to 2.5 in 2 L freshly prepared -ura galactose media at 30°C and 120 rpm.

3.4.2 Spheroplast preparation

After the desired OD₆₀₀ was obtained, cells were harvested by centrifugation at 5000 rpm for 5 min at 4°C on a Sorvall RC 6 Plus centrifuge using an SLC-3000 rotor. In order to estimate the cell wet weight, the resulting cell pellet was washed with distilled water and centrifuged

again by using the same parameters as before. After determination of the cell wet weight, the pellet was resuspended in prewarmed DTT buffer (2 mL/g cell wet weight) and incubated for 20 min at 30°C with shaking at 120 rpm. After centrifugation at 4000 rpm for 5 min at 4°C on a Sorvall RC 6 Plus centrifuge using a SLC-3000 rotor, the resulting pellet was washed with approximately 100 mL zymolyase buffer (without enzyme). In order to convert the cells to spheroplasts, the resulting pellet was resuspended in prewarmed zymolyase buffer (7 mL/g cell wet weight, without enzyme) and 50 µL of the treated yeast suspension were mixed with 2 mL distilled water for the zymolyase test. Afterwards 3 mg zymolyase per g cell wet weight were added to the yeast suspension, and incubated for 30 min at 30°C with shaking at 120 rpm. Spheroplast building was monitored by adding 50 µL cell suspension into 2 mL distilled water. A clear lysate confirmed the successful spheroplast building. Spheroplasts were harvested at 4000 rpm for 5 min at 4°C on a Sorvall RC 6 Plus centrifuge using a SLC-3000 rotor. Finally, the resulting pellet was washed with zymolyase buffer (without enzyme) and centrifuged at 3000 rpm for 5 min at 4°C using the same centrifuge and rotor as before.

3.4.3 Isolation of mitochondria

The following steps were performed on ice. The resulting spheroplasts were resuspended in homogenizing buffer (6.5 mL/g cell wet weight) with PMSF (final concentration of 1 mM) and homogenized 15 times using a Dounce homogenizator and a tight fitting pistil. The homogenized cell suspension was centrifuged at 3000 rpm for 5 min at 4°C on a Sorvall RC 6 Plus centrifuge using a SS-34 rotor. Supernatants were collected and samples were taken from homogenate and stored at -70°C for further analyses. The remaining homogenate was centrifuged at 4000 rpm for 10 min at 4 °C using the same centrifuge and rotor as before. In a second centrifugation step at 12000 rpm for 15 min at 4°C, using a Sorvall RC 6 Plus

centrifuge and a SS-34 rotor, the resulting supernatant was again sedimented, leading to crude mitochondria pellets. Crude mitochondria pellets were resuspended in 1 mL SEM buffer and combined in a SS-34 centrifugation tube. Afterwards the tube was filled up with SEM buffer to $\frac{3}{4}$ of the total volume and centrifuged using the same centrifugation procedure as before. The resulting mitochondria pellet was resuspended in SEM buffer (500-1000 μ L) and 40 μ L aliquots were shock frozen with liquid N₂.

Table 24: Composition of all buffers used for spheroplast and mitochondria preparation

Buffer	Component
DTT-Buffer	10 mM DTT 0.1 M Tris/H ₂ SO ₄ pH 9.4
Zymolyase-Buffer	1.2 M Sorbitol 20 mM KH ₂ PO ₄ pH 7.4 (with KOH)
Homogenizing-Buffer	44 g sorbitol 484 mg Tris 150 mg EDTA 0.8 g BSA ad 400 mL monodest. H ₂ O pH 7.4 (with HCl)
SEM-Buffer	42.8 g saccharose 1.05 g MOPS 186 mg EDTA add 500 mL monodest. H ₂ O pH 7.2 (with KOH)

3.5 Analytical methods

3.5.1 Protein Analyses

3.5.1.1 Protein precipitation and quantification

Protein quantification was performed by the method of Lowry et al. (1995) with minor modifications.

Subcellular fractions were diluted with distilled water (homogenate 1:10; mitochondria 1:10 or 1:5, depending on the sample density). 25 μL and 50 μL of each sample were added to distilled water to a final volume of 400 μL . After adding 100 μL of 50% (w/v) ice cold TCA to initiate protein precipitation, all samples were incubated for at least 1 h on ice. Proteins were sedimented by centrifugation at 13000 rpm for 10 min at 4°C (Heraeus FRESCO 17), and the aqueous supernatant was removed. The resulting protein pellets were washed with ice cold distilled water and solubilized in 100 μL solution C (Table 25) for 30 min at 65°C. Dissolved samples were transferred into glass tubes containing 300 μL H₂O and 2 mL of solution A (Table 25). After incubation for 10 min at RT, 200 μL of solution B (Table 25) were added to each sample. Absorption was measured at a wavelength of 546 nm with a Hitachi U-1100 UV/VIS spectrophotometer after 30 min. For calculating the protein concentration of each sample, a standard curve was generated by using serum albumin as a standard.

Table 25: Solutions for protein precipitation and quantification

Solution	Component
Solution A	0.96% (v/v) of 2.2% Na ₂ -Tartrat 0.96% (v/v) of 1% CuSO ₄ *5H ₂ O 2.39%(v/v) of 20% SDS 95.69 (v/v) of 2% Na ₂ CO ₃ in 0.1 M NaOH
Solution B	Folin-Ciocalteu-Phenol Reagent 1:2 diluted with H ₂ O
Solution C	0.1% SDS in 0.1 M NaOH

3.5.1.2 SDS-PAGE

After protein quantification, volumes of each fraction that correspondent to 0.2 mg protein were transferred into Eppendorf tubes. After adding distilled water to a final volume of 400 μL , protein precipitation was performed as described in 3.5.1.1. The resulting protein pellets were resuspended in 100 μL sample buffer (Table 26) and incubated for 30 min at 37°C,

leading to samples with a final protein concentration of 2 µg/µL. After denaturation at 95°C for 3 min samples were used for SDS-PAGE or stored at -20°C.

Table 26: Solutions for SDS-PAGE

Solution	Component
TCA	50% (w/v) trichloroacetic acid
Dissociation buffer	20 mM KH ₂ PO ₄ , pH 6.8 6 mM EDTA 6% SDS 10% Glycerol 0.05 Bromphenol Blue
Sample buffer	73% H ₂ O 25% Dissociation buffer 1% PMSF 1% Mercaptoethanol

Sodiumdodecylsulphate polyacrylamide gel electrophoresis (SDS-PAGE) is a method for separating proteins according to their electrophoretic mobility. SDS-PAGE was carried out as described by Laemmli (1970) using BioRad Mini Protean II equipment. The 5% stacking gel was responsible for concentrating proteins, which subsequently were separated according to their molecular weight in the 12.5% separating gel. Additionally a gradient gel consisting of a 5% stacking and a 12.5%-18% separation gel was used (Table 27). 5 µL of protein standard (Fermentas PageRuler™ Prestained Protein Ladder; 170, 130, 100, 70, 55, 40, 35, 25, 15, and 10 kDa) as well as 10-20 µg protein of each fraction were loaded on the SDS gels. The SDS-PAGE was carried out at 42 mA for approximately 90 min. Afterwards the gels were used for Western Blot analysis.

Table 27: Components for PAGE stacking and separating gels

Component	Volume [μL]		
	5% Stacking gel	12.5% separation gel	18% separation gel
dist. H ₂ O	3690	2990	1620
1 M Tris/HCl, pH 6.8	625	-	-
1 M Tris/HCl, pH 8.8	-	3750	3750
40% Acrylamide/ 0.8% Bisacrylamide	562.5	3120	4490
20% SDS	25	50	50
10% (NH ₄) ₂ S ₂ O ₈	25	48	48
TEMED	5	10	10

Table 28: Running buffer for SDS-PAGE

Component	Amounts [g]
Tris	3
EDTA	0.334
Glycine	14.2
SDS	0.08
dist. H ₂ O	1000

3.5.1.3 Western Blot analysis

Western Blot analysis was used for quality control of isolated fractions and for localization studies. According to Haid and Suissa (1983) separated proteins were transferred from the gels of the SDS-PAGE (3.5.1.2) to nitrocellulose membranes (Hybond C, 0.45 micron) with a Trans-Blot apparatus at 220 mA for 1 h. The success of protein transfer could be verified by staining the nitrocellulose membrane with water soluble PonceauS dye.

Table 29: Transfer buffer for protein transfer

Component	Volume [mL]
10 x Blotting Buffer	100
Methanol	200
dist. H ₂ O	700
20% SDS	0.5

Table 30: 10 x Blotting Buffer

Component	Amount [g]
Tris	3
Glycine	14
dist. H ₂ O	1000

In order to saturate all free protein binding sites, the membrane was incubated with whey proteins (solution A) for 1 h at RT or overnight at 4°C on a shaker. Excess of whey proteins was removed by washing the membrane with Tris buffer containing Triton (TBST buffer). Then the membrane was incubated with the first antibody dissolved in solution B for 1 h at RT on a shaker. The membrane was washed three times with TBST buffer for 10 min, each, at RT on a shaker. Afterwards, the membrane was exposed for 1 h at RT to the peroxidase-linked second antibody dissolved in solution B (1:5000). The membrane was washed twice with TBST buffer for 10 min, each, at RT and rinsed once with TBS buffer. Antibody-antigen complexes were visualized by chemiluminescence using Luminata™ Classico Western Blot HRP Substrate. Specific proteins were detected by exposing the membrane to X-ray films (Ortho G Kodak film). The film was developed by using two photochemical solutions (Kodak) starting with incubating the film in a developer solution for approximately 30 sec, washing in water and incubating in a fixing solution for approximately 1 min. Finally, the film was washed with water and dried. Used solutions and antibodies are listed in Table 31-32.

Table 31: Solutions for Western Blotting

Solution	Component
TBS buffer	50 mM Tris 150 mM NaCl pH 8.0 (with HCl)
TBST buffer	TBS Solution 0.5% of 20% Triton X-100
Solution A	TBS buffer 5% milk powder
Solution B	TBS buffer 2.5% milk powder

Table 32: Primary and secondary antibodies used for detection of Psd1

Antibody systems			
Primary antibody	Marker	Secondary antibody	Marker
Psd1 β	β -subunit of Psd1	Anti-rabbit POD	Anti-rabbit Ig with horse radish peroxidase
HF Anti-HA POD	α -subunit of Psd1 coupled to horse radish peroxidase	-	-
Tom70	OMM protein Tom70	Anti-rabbit POD	Anti-rabbit Ig with horse radish peroxidase
Tim44	matrix protein Tim44		
Tim23	IMM protein Tim23		

3.5.2 Submitochondrial localization of proteins and solubility studies

3.5.2.1 Submitochondrial localization studies

The submitochondrial localization of Psd1 was determined by treating intact, hypotonically swollen or lysed mitochondria with proteinase K (Figure 18). In general, hypo-osmotic swelling of mitochondria was performed by treating mitochondria with a 19:1 ratio of EM buffer (10 mM MOPS-KOH (pH 7.2) and 1 mM EDTA) and SEM buffer (Table 24) for 10 min on ice, creating mitoplasts. Afterwards the samples were treated with 20 μ g/mL proteinase K for 15 min on ice. For lysis, mitochondria were treated with Triton X-100 at a final concentration of 0.5% (v/v) prior to addition of proteinase K. Proteinase K activity was stopped by adding 2 mM PMSF and incubation for 10 min on ice. Subsequently, mitochondria were re-isolated by centrifugation for 10 min at 13000 rpm and 4 °C and washed with SEM buffer.

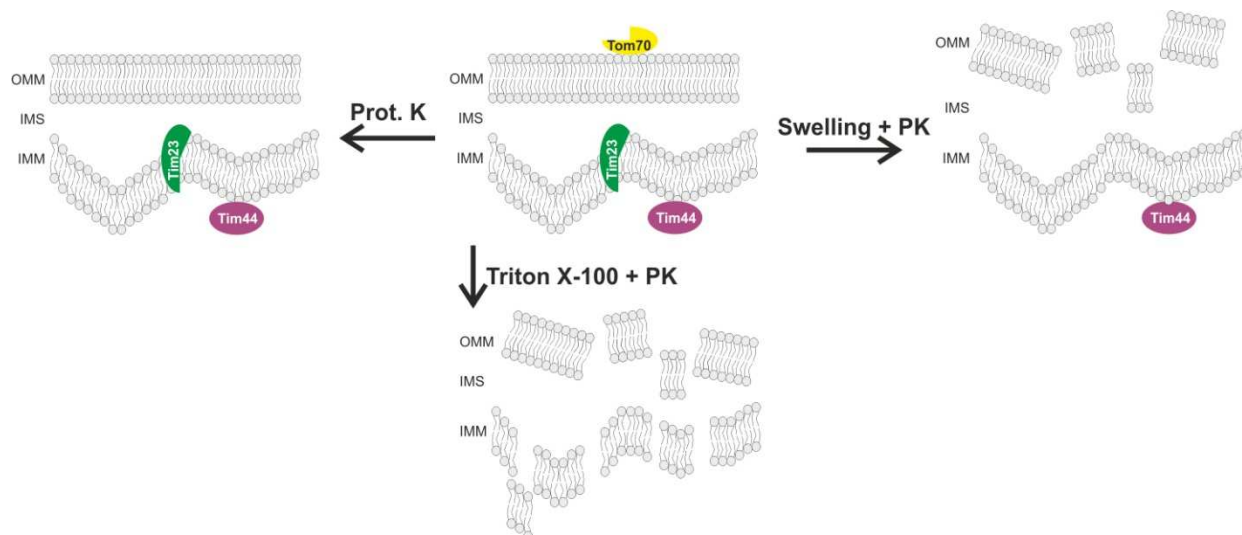


Figure 18: Scheme of submitochondrial localization studies

Finally, the samples were subjected to SDS-PAGE and Western Blot analysis as described above. In addition to the Psd1 specific antibodies against the β -subunit and the HA-tagged α -subunit, antibodies against mitochondrial marker proteins located at the OMM (Tom70), facing the IMS (Tim23) or in the matrix (Tim44) were used (Table 32). This special set of antibodies was used to determine the submitochondrial localization of the Psd1 variants.

3.5.2.2 Carbonate extraction

Carbonate extraction was used to determine the membrane integration of Psd1 mutant variant proteins by treating mitochondria with freshly prepared carbonate buffer (Na_2CO_3) at pH 11.5. Under these conditions soluble and membrane associated proteins are extracted, whereas membrane bound proteins remain in the pellet.

For the carbonate extraction, 70 μg of isolated mitochondria were resuspended in 200 μL of freshly prepared 0.1 M Na_2CO_3 buffer (pH 11.5) and incubated for 30 min on ice. Subsequently, the samples were centrifuged for 40 min at 125000 g and 4°C using an Optimis™ Max ultracentrifuge (Beckman) and a TLA55 rotor. The remaining pellet was

immediately dissolved in 50 μ L sample buffer (Table 26), whereas the supernatant was subjected to TCA precipitation as describe in 3.5.1.1. As a control sample (total sample), 70 μ g of isolated mitochondria were resuspended in 200 μ L of 0.1 M carbonate buffer, incubated for 30 min on ice and subjected to TCA precipitation. The resulting pellet was again dissolved in 50 μ L sample buffer. Samples (total, pellet and supernatant) were used for SDS-PAGE and Western Blot analysis employing Psd1 specific antibodies against the β -subunit and the HA-tagged α -subunit, as well as antibodies against the soluble mitochondrial matrix protein Tim44 and the integral mitochondrial outer membrane protein Porin (Table 33). The control proteins Tim44 and Porin allowed a reliable conclusion about the membrane association and solubility of the Psd1 variants.

Table 33: Primary and secondary antibodies used for detection of Psd1, Tim44 and Porin

Antibody systems			
Primary antibody	Marker	Secondary antibody	Marker
HF Anti-HA POD	α -subunit of Psd1 coupled to horse radish peroxidase	-	-
Psd1 β	β -subunit of Psd1	Anti-rabbit POD	Anti-rabbit Ig with horse radish peroxidase
Por1p	Porin		
Tim44	matrix protein Tim44		

3.5.3 Phospholipid analyses

3.5.3.1 Lipid extraction from mitochondria and homogenate fractions

Lipids from mitochondrial and homogenate fractions of wild type and mutant strains grown to the early exponential growth phase (0.8-1.5) were extracted by the method of Folch (1957). Lipids were extracted from 1 mg mitochondria and 2-3 mg homogenate with 4 mL chloroform/methanol (2/1; v/v) in a Pyrex glass tube. After extraction for 1 h under shaking on a Vibrax VXR basic with 1500 rpm, 2 mL of 0.034% MgCl₂ solution (w/v) were added, and samples were again vortexed for 30 min. Subsequently, the samples were centrifuged for 3

min at 1500 rpm and RT on a table top centrifuge (Hettich Rotina 46 R) and the upper aqueous phase as well as the protein containing interphase were removed. The remaining organic phase was washed with 2 mL 2 N KCl/methanol (4/1; v/v) and vortexed for 10 min. Afterwards, the samples were again centrifuged as describe above and the upper aqueous phase was removed by vacuum. After repeating this washing step, 1.5 mL of an artificial upper phase, containing methanol/H₂O/chloroform (48/47/3; v/v/v), as added to the organic phase. Subsequently, the samples were vortexed for 10 min and centrifuged for 5 min at 1500 rpm and RT. After removing the upper aqueous phase, the remaining organic phase was dried under a steam of nitrogen.

3.5.3.2 Lipid analysis by two dimensional thin layer chromatography

The extracted lipids were dissolved in 50 µL chloroform/methanol (2/1; v/v) and spotted onto a Silica gel 60 plate (10 x 10, Merck, Darmstadt, Germany) using a Hamilton[®] Microliter syringe. Individual phospholipids were separated using two developing solvent systems. For the first dimension the solvent contained chloroform/methanol/25% NH₃ (68/35/5; per vol.) and for the second dimension it contained chloroform/acetone/methanol/acetic acid/H₂O (53/20/10/10/5; per vol.) Chromatograms were developed in an ascending manner to the top of the plate for 50 min using the first solvent system. After drying, plates were turned for 90° and developed in the second dimension to the top of the plate for 45 min using the second solvent system. Subsequently, the plates were dried and lipids were visualized by iodine vapour. Separated phospholipids were marked with a pencil.

3.5.3.3 Phospholipid determination

Phospholipids were quantified by the method of Broekhuysse (1968). Separated phospholipids (3.5.3.2) were scraped off the plate and transferred into phosphate-free glass tubes. After a drying step at 100°C for 15 min, 0.2 mL of an acidic mixture (Table 34) were added. Subsequently, samples were heated at 180°C for 30 min on a heating block. Then, samples were cooled down in a fume cupboard and 4.8 mL of solution I/solution II (Table 34) at a ratio of 500:22 were added. The reaction was initiated by heating the samples in tubes, which were closed with stoppers and clamps at 100°C for 30 min. After incubation, samples were centrifuged for 3 min at 1500 rpm and RT, using a table top centrifuge (Hettich Universal 16). Samples were measured at 830 nm using a Hitachi U110 UV/VIS spectrometer.

Table 34: Solutions for phospholipid determination

Acidic mixture	Solution I	Solution II
90 vol% conc. H ₂ SO ₄ 10 vol% 72 HClO ₄	0.26% (NH ₄) ₆ Mo ₇ O ₂₄ *4*H ₂ O	0.16 g/mL K ₂ S ₂ O ₅ 2.52*10 ⁻³ g/mL ANS acid. 5*10 ⁻³ g/mL Na ₂ SO ₃

3.5.4 Enzymatic activity assay

The activity of Psd1 was determined by measuring [H³]PE synthesis from [H³]PS (substrate, specific activity: 1424 dpm/nmol) in mitochondrial fractions of Psd1 mutants and wild type. For the enzymatic reaction 100 nmol of radioactively labelled substrate was transferred to a glass tube and dried under a steam of nitrogen. 500 µL Psd1 buffer (Table 35) was added and substrate-liposomes were generated by sonication for 7 min using an ultrasonic bath (Transsonic 420, Elma®). After sonication the glass tubes were placed in a water bath (30°C) and samples were stirred. Meanwhile, a sample of mitochondria corresponding to an amount of 1 mg protein was diluted with SEM buffer to a final volume of 1 mL (Table 36). The enzymatic reaction was started by adding 1 mL sample to 500 µL of the previously

prepared substrate. The enzymatic reaction was monitored for 7 min by taking samples at 0.5, 1.5, 2.5, 3.5, 5 and 7 min. The reaction was stopped with chloroform/methanol (2/1; v/v) and lipids were extracted as described (3.5.3.1).

Table 35: Solutions for enzymatic activity assay

Buffer	Component
SEM Buffer	42.8 g saccharose 1.05 g MOPS 186 mg EDTA add 500 mL monodest. H ₂ O pH 7.2 (with KOH)
Psd1 Buffer	0.2 M Tris/HCl 20 mM EDTA pH 7.4 (with HCl)

Dried lipid extracts were dissolved in 50 μ L chloroform/methanol (2/1; v/v) and spotted onto a Silica gel 60 plate (10 x 20, Merck, Darmstadt, Germany) using a Hamilton[®] Microliter syringe. Phospholipids were separated using two developing solvent systems in one dimension. The first system contained chloroform/methanol/25% NH₃ (50/25/5; per vol.) and the second chloroform/acetone/methanol/acetic acid/H₂O (53/20/10/10/5; per vol.). Chromatograms were developed in an ascending manner to the top of the plate for 50 min using the first solvent system. After drying, plates were developed in the same dimension for 45 min using the second solvent system. Subsequently the plates were exposed to iodine vapour and lipids were visualized. Separated phospholipids were marked with a pencil.

[H³]PE synthesis from [H³]PS was measured by scrapping off spots of PE. Samples were transferred to LSC tubes and suspended in 8 mL LSC Safety Scintillation Cocktail (J. T. Baker, Deventer, The Netherlands) containing 5% water (v/v). After mixing on a Vortex Genie 2 and incubation for 1 h, radioactivity was counted with a TRI-CARB 29000 TR Liquid Scintillation Analyser (Packard) using the protocol for determining [H³] samples with water.

4 Results

4.1 Dissection of Psd1 into specific domains

According to the online transmembrane prediction programs DAS and TMpred, the mitochondrial enzyme phosphatidylserine decarboxylase 1 contains two hydrophobic regions (Figure 19). Both predicted transmembrane helices are formed by approximately 20 amino acids between amino acids 80 to 100 (IM1) and 120 to 140 (IM2), respectively. A mutant variant strain expressing *PSD1* lacking the first predicted transmembrane region has already been investigated (Horvath et al., 2012).

To analyze specific domains within the Psd1 sequence, their function and their molecular properties, two mutants lacking the second predicted transmembrane domain and both predicted transmembrane domains were cloned. Moreover, a third Psd1 construct lacking the potential substrate recognition site within the α -subunit of the protein was generated. These mutants were cloned by overlap-extension-PCR and transformed into *E. coli*. Positive clones were identified by restriction analysis and sequencing. Verified plasmids were transformed into *psd1* Δ yeast strains and positive transformants were confirmed by colony-PCR.

The 57 kDa primary translation product of Psd1 undergoes three processing steps during import into mitochondria leading to a 4 kDa α -subunit and a 46 kDa β -subunit. To monitor both Psd1 subunits independently, yeast strains expressing Psd1 with an HA-tag C-terminally fused to the α -subunit were generated and a specific antibody recognizing the β -subunit (Psd1 β) was used (Figure 19).

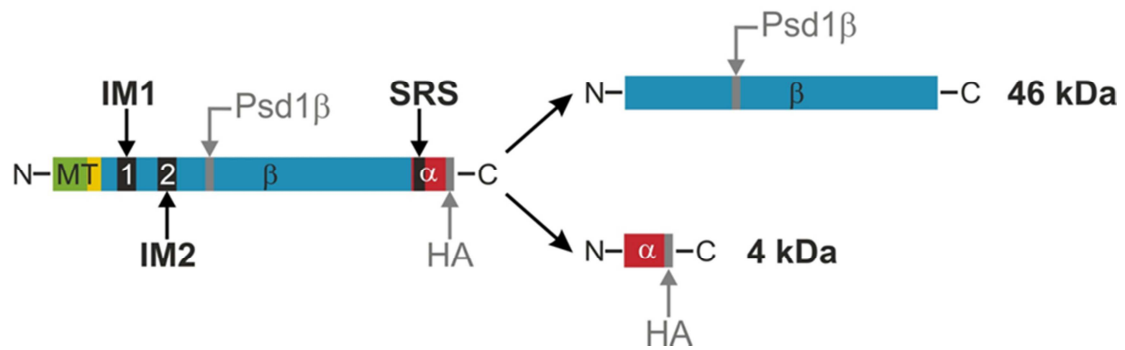


Figure 19: Specific domains and antibody recognition sites of Psd1

Wild type and mutant strains were grown to the early logarithmic growth phase and mitochondria were isolated and subsequently subjected to SDS-PAGE and Western Blot analysis (Figure 20).

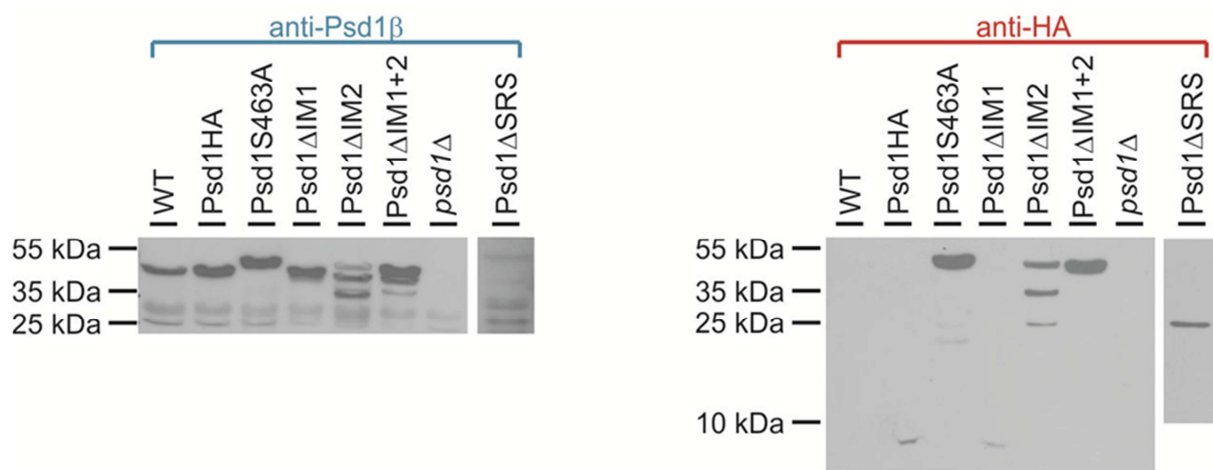


Figure 20: Western blot analysis of Psd1 mutants. The anti-Psd1 β antibody recognize the β -subunit of Psd1, whereas the anti-HA antibody recognize the α -subunit of the enzyme.

Besides Psd1 Δ IM2, Psd1 Δ IM1+2 and Psd1 Δ SRS, also the Psd1 mutants Psd1HA, Psd1 Δ S463A and Psd1 Δ IM1 generated by Horvath et al. (2012) were subjected to SDS-PAGE and Western Blot analysis and used as comparative samples. The domains of the Psd1 mutants and wild type Psd1 are shown in Figure 21. Psd1 mutants comprise an HA-tag C-terminally fused to the α -subunit, permitting its detection with an anti-HA antibody.

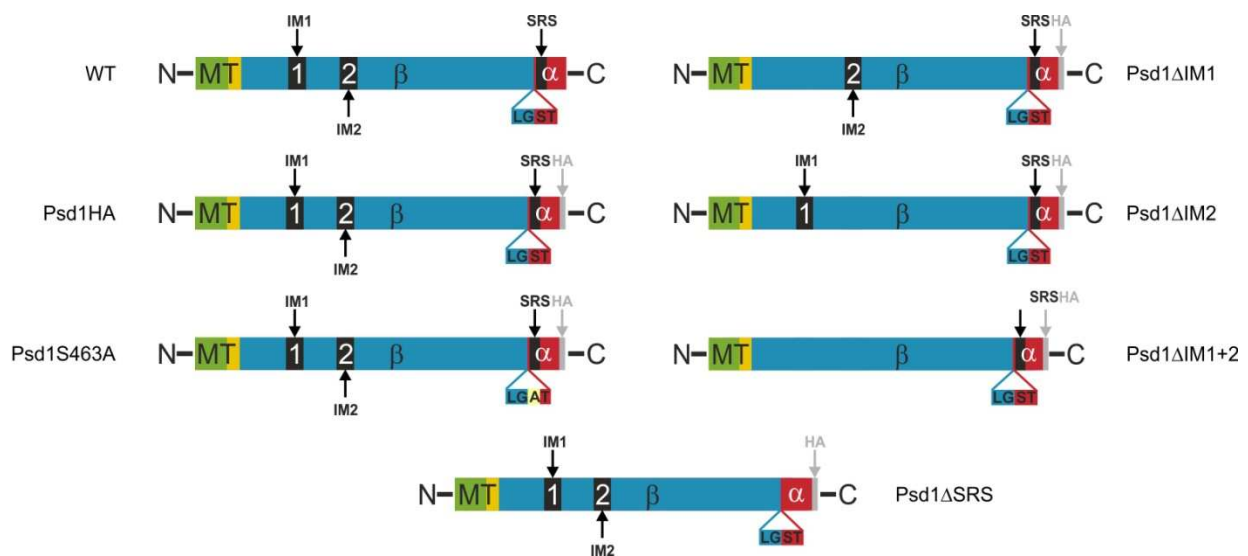


Figure 21: Domains of the wild type (WT) and the Psd1 mutants (Psd1HA, Psd1S463A, Psd1ΔIM1, Psd1ΔIM2, Psd1ΔIM1+2 and Psd1ΔSRS)

Apart from Psd1S463A, the Psd1 mutants and wild type Psd1 display a LGST motif, which is the site of autocatalytic processing of the enzyme. In Psd1S463A a single mutation of serine 463 to alanine within this motif leads to impaired cleavage of Psd1 into α - and β -subunits.

Western Blot analysis (Figure 20) showed a single protein band for the wild type Psd1, Psd1HA and Psd1ΔIM1 after reaction with the Psd1 β antibody. The size of the intact β -subunit of Psd1 upon autocatalytic processing corresponded to 46 kDa. For Psd1S463A a 50 kDa intermediate was detected, representing Psd1 before autocatalytic processing into an α - and a β -subunit. However, the results for Psd1ΔIM2 and Psd1ΔIM1+2 were unexpected. Psd1ΔIM2 showed two fragments smaller than 46 kDa. In contrast, Psd1ΔIM1+2 displayed three fragments, one with a size of 46 kDa and two smaller ones. The additional protein fragments might represent degradation products of Psd1 (Figure 20).

To address the ability of Psd1ΔIM2 and Psd1ΔIM1+2 to undergo autocatalytic cleavage at the LGST motif, Western Blot analysis by using the high affinity HA-antibody recognizing the α -subunit (4 kDa) were performed. Previous studies (Horvath et al., 2012) described that Psd1ΔIM1 acts like wild type Psd1 (Psd1HA) regarding autocatalytic processing into an α - and

a β -subunit. In contrast, Psd1S463A was not able to perform autocatalytic cleavage into an α - and a β -subunit, and a 50 kDa intermediate was detected.

Psd1 Δ IM2 showed three and Psd1 Δ IM1+2 one Psd1 intermediate using the anti-HA antibody. Comparing results obtained for Psd1S463A, Psd1 Δ IM2 and Psd1 Δ IM1+2 revealed that deletion of the second predicted transmembrane domain caused Psd1 fragmentation leading to fragments smaller than 50 kDa. Furthermore, Psd1 lacking IM2 was not autocatalytically cleaved but N-terminally degraded during mitochondrial import. Deletion of the proposed substrate recognition site within the α -subunit displayed the strongest effect on Psd1 maturation. Psd1 Δ SRS was N-terminally degraded, autocatalytic cleavage was inhibited and a 26 kDa fragment was detected with an antibody against the C-terminal located HA-tag.

4.2 Submitochondrial localization of Psd1 Δ IM2, Psd1 Δ IM1+2 and Psd1 Δ SRS

Recent studies have shown that Psd1 is anchored to the inner mitochondrial membrane *via* the first predicted transmembrane domain located within the β -subunit, whereas the α -subunit is protruding into the intermembrane space as soluble part of the protein (Horvath et al., 2012). To study the effect of each transmembrane domain and the potential substrate recognition site on the submitochondrial localization of both Psd1 subunits, hypo-osmotic swelling experiments were performed with Psd1 Δ IM2, Psd1 Δ IM1+2 and Psd1 Δ SRS. In these experiments intact, hypotonically swollen or lysed mitochondria were treated with proteinase K and subsequently investigated through Western Bot analysis with antibodies against the β -subunit, the α -subunit (HA-tag) and control proteins Tom70, Tim44 and Tim23.

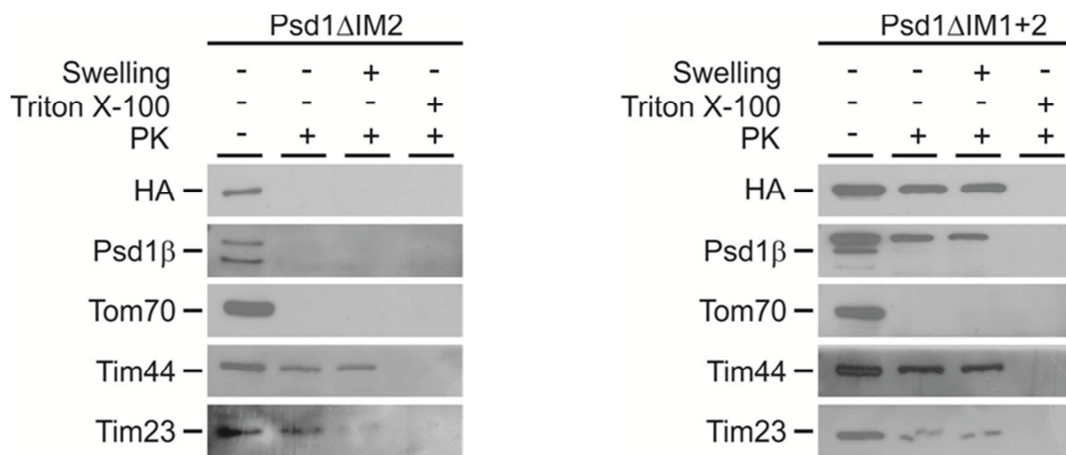


Figure 22: Western Blot analysis of Psd1ΔIM2 and Psd1ΔIM1+2 upon hypo-osmotic swelling

Figure 22 shows that both subunits of Psd1ΔIM2 were degraded by proteinase K on intact mitochondria. Similarly, the outer mitochondrial membrane protein Tom70 was proteolytically cleaved on intact mitochondria. The inner membrane protein Tim23 with the antibody recognition site facing the intermembrane space was degraded only after rupture of the outer membrane by hypo-osmotic swelling, whereas the matrix localized Tim44 was digested only after lysis of mitochondria with detergent. These results indicate that Psd1ΔIM2 is localized at the outer mitochondrial membrane. We can speculate that the first predicted transmembrane domain functions as membrane anchor whereas the second transmembrane domain might be important for Psd1 localization to the inner mitochondrial membrane.

Localization experiments of Psd1ΔIM1+2 showed that both subunits were only digested after lysis of mitochondria with detergent similar to the matrix located Tim44. This Psd1 variant is therefore localized to the matrix fostering the theory of the first transmembrane domain being a membrane anchor of the protein (Figure 22).

Localization experiments of Psd1 Δ SRS did not yield clear results. Similar to the outer transmembrane protein Tom70, the α -subunit was degraded by proteinase K on intact mitochondria. Since it was already demonstrate that Psd1 Δ SRS is N-terminally degraded including the anti-Psd1 β antibody recognition site, it was impossible to obtain clear information about the localization of the β -subunit. The inner membrane protein Tim23 was degraded on intact mitochondria, whereas the matrix localized Tim44 was digested only after lysis of mitochondria with detergent (Figure 23).

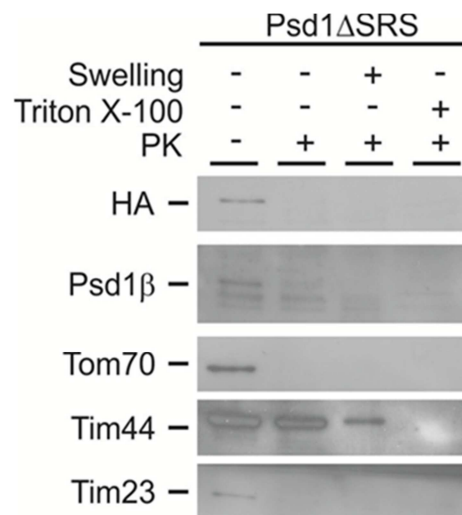


Figure 23: Western Blot analysis of Psd1 Δ SRS upon hypo-osmotic swelling

Since it was assumed that the proteinase K concentration used in this experiments or the established hypo-osmotic swelling conditions might be responsible for the unclear results obtained with Psd1 Δ SRS, two more experiments were performed. First, intact mitochondria were treated with different amounts of proteinase K showing that already a low concentration of proteinase K caused degradation of the outer membrane protein Tom70 and the inner membrane protein Tim23, without affecting the matrix protein Tim44. Second, mitochondria were treated with a steady concentration of proteinase K (1000 μ g/mL) and the strength of hypo-osmotic swelling was constantly increased by adding more swelling buffer (EM buffer). This displayed that Tom70 and Tim23 were already digested on intact

mitochondria (no EM added), whereas Tim44 remained intact (Figure 24). The results indicate that mitochondria isolated from strains expressing Psd1 Δ SRS exhibit a malfunctioning outer membrane system leading to permeability of the outer mitochondrial membrane for proteinase K.

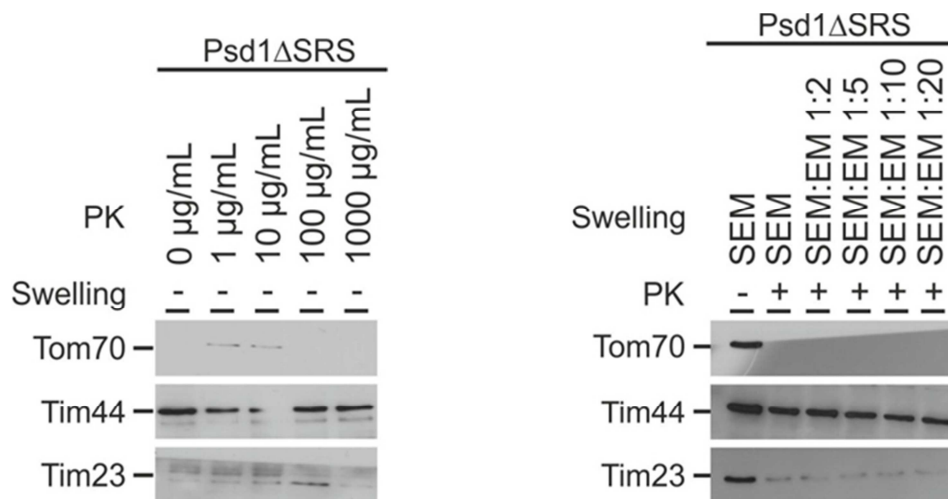


Figure 24: Additionally Western Blot analysis of Psd1 Δ SRS. The left figure shows treatment of intact mitochondria with different amounts of proteinase K. The left figure shows steady proteinase K treatment of mitochondria for which the strength of hypo-osmotic swelling was constantly increased by adding more swelling buffer.

4.3 Psd1 is anchored to the inner mitochondrial membrane by IM1

The β -subunit anchors Psd1 to the inner mitochondrial membrane (Horvath et al., 2012). Both subunits, α and β , are attached to each other after autocatalytic processing. The α -subunit remains in the supernatant after carbonate extraction and is the soluble part of the protein. To investigate the membrane integration of Psd1 mutants lacking transmembrane domain 2 (IM2) or the substrate recognition site carbonate extraction was used. According to this method integral membrane proteins stay in the pellet and soluble proteins are extracted under these conditions. To test membrane integration Psd1 Δ IM2, Psd1 Δ IM1+2 and Psd1 Δ SRS were subjected to carbonate extraction at pH 11.5. Subsequent Western Blot

analysis was performed with antibodies against the Psd1 β -subunit (Psd1 β), the HA-tagged α -subunit (HA) and mitochondrial control proteins.

All intermediates of Psd1 Δ IM2 which is impaired in autocatalytic processing remained in the pellet (P) after carbonate extraction at pH 11.5. Similar results were obtained for the membrane protein porin, whereas the peripheral soluble protein Tim44 was efficiently removed (Figure 25). However, Psd1 Δ IM1+2 was detected in the pellet as well as in the supernatant upon alkaline extraction, indicating that this Psd1 variant is partially soluble (Figure 25). As Psd1 Δ IM2, Psd1 Δ IM1+2 is also impaired in processing into an α - and a β -subunit.

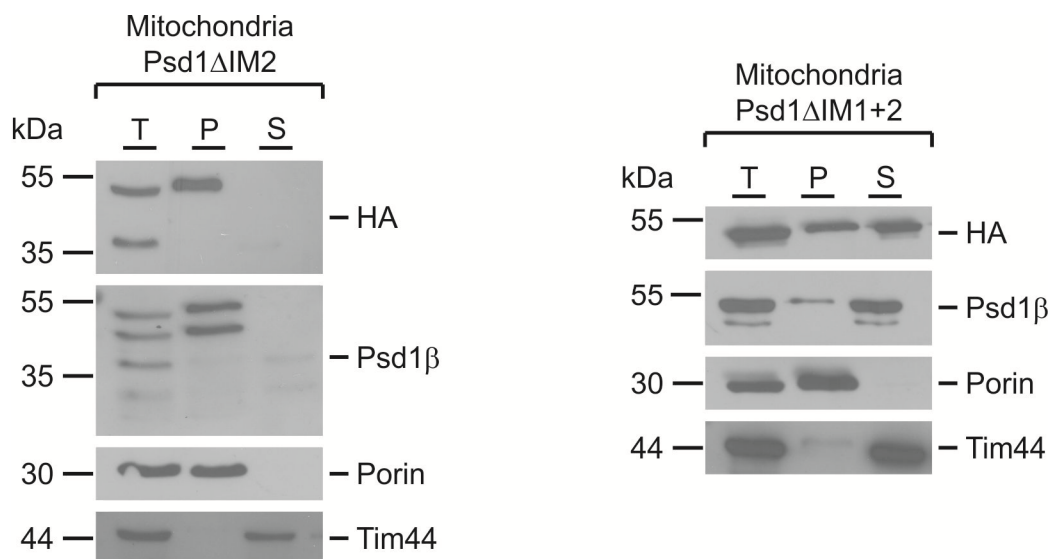


Figure 25: Western Blot of analysis of Psd1 Δ IM1 and Psd1 Δ IM2 upon carbonate extraction

Carbonate treatment of Psd1 Δ SRS showed partial solubility of degradation products with the size of 35 kDa. In this Psd1 variant, maturation into α - and β -subunits was inhibited. Intermediates with a size of 50 kDa and 26 kDa remained in the pellet after alkaline extraction at pH 11.5, whereas the peripheral soluble protein Tim44 was efficiently removed (Figure 26).

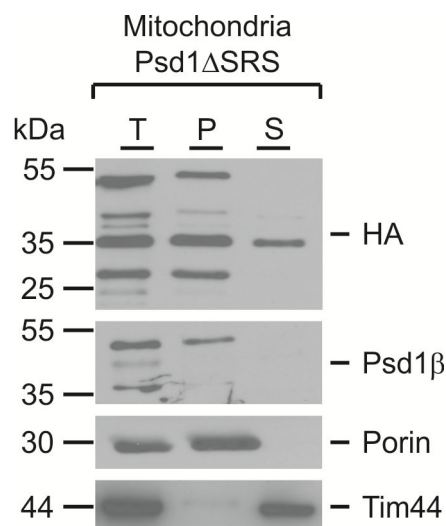


Figure 26: Western Blot of analysis of Psd1 Δ SRS upon carbonate extraction

These results and the previously performed swelling experiments showed that Psd1 Δ IM2 contains a membrane anchor tethering the entire protein including the α -subunit to the outer mitochondrial membrane. In contrast Psd1 Δ IM1+2 is partially soluble and faces the mitochondrial matrix. Carbonate extraction and swelling of Psd1 Δ SRS revealed instability of the protein which features membrane bound as well as membrane associated degradation products. The solubility of the degradation products strongly depends on the excess of N-terminally degradation. Mutants lacking either the second predicted transmembrane domain (IM2) or the substrate recognition site (SRS) have one common feature: they are impaired in autocatalytic processing to α - and β -subunits.

4.4 Functionality of wild type Psd1 and Psd1 variants

4.4.1 Impaired Psd1 processing causes loss of enzymatic activity

Localization and solubility studies have shown that the predicted transmembrane domains as well as the potential substrate recognition site are important for correct topology and processing of Psd1 (Horvath et al., 2012; see 4.2; 4.3). To investigate the effect of Psd1 mislocalization on enzymatic activity, Psd1 Δ IM2, Psd1 Δ IM1+2 were subjected to

phosphatidylserine decarboxylase activity assays using [³H]-labeled PS. Samples were incubated with [³H]PS and formation of [³H]PE was measured by liquid scintillation counting (LSC) after lipid extraction and chromatographic separation. Psd1 activity was determined by plotting the dpm values against the corresponding time points (Figure 27) and by applying the following equation (Table 36):

$$Psd1 \text{ activity} = \frac{k \text{ (slope of trend lines)}}{\text{specific activity} * \text{mitochondrial protein amount}}$$

Table 36: Determination of Psd1 activity

	Specific activity [dpm/nmol]	Mitochondrial protein amount [mg]	k (slope) [dpm/min]	Psd1 activity [nmol/min*mg]
Wild type (WT)	1424	0.133	754.6	3.97
Psd1ΔIM2	1424	0.133	-17.5	n. d
Psd1ΔIM1+2	1424	0.133	-0.10	n. d
Psd1ΔSRS	1424	0.133	-10.5	n. d

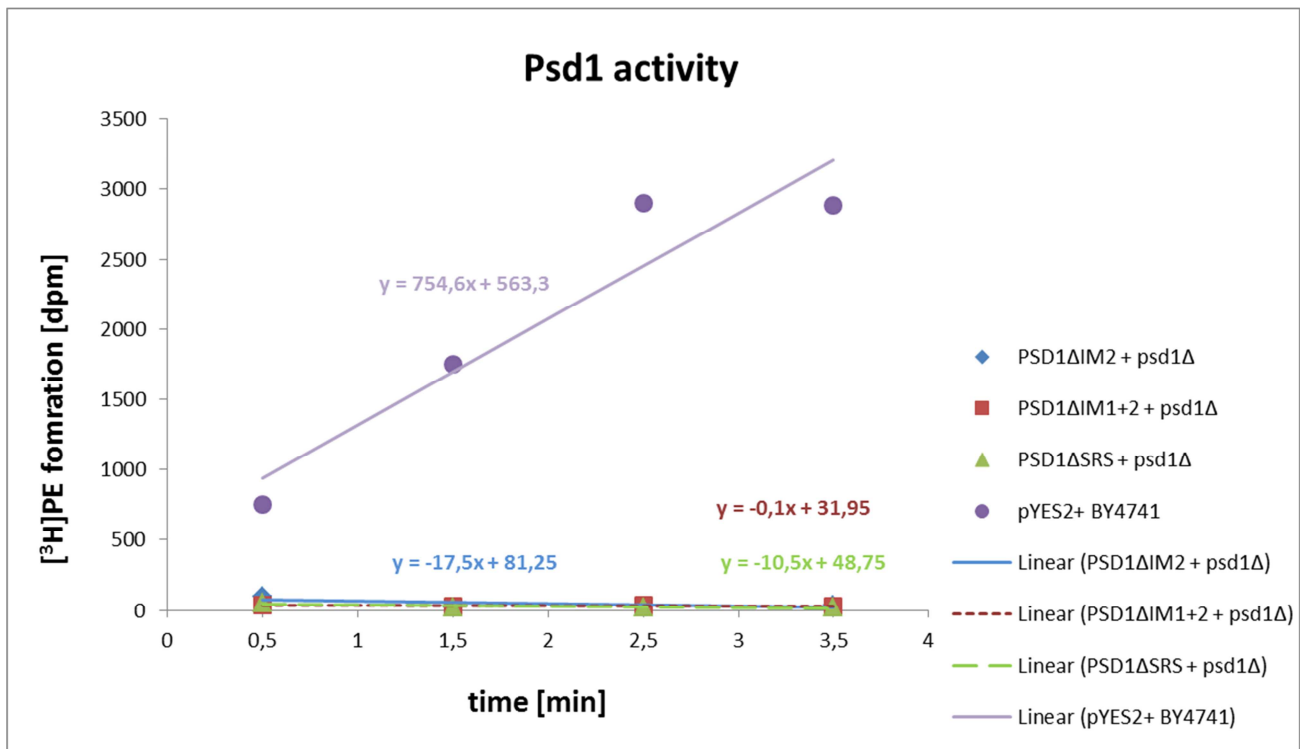


Figure 27: Plot of the measured dpm values against the time

In comparison to wild type Psd1, Psd1 lacking the second transmembrane domain alone (Psd1 Δ IM2) or in combination with the first transmembrane domain (Psd1 Δ IM1+2), displayed no detectable decarboxylase activity. The reason for the observed enzyme inactivity can be explained by the inability of Psd1 Δ IM2 and Psd1 Δ IM1+2 to undergo autocatalytic cleavage, which is essential for the generation of the active site of the enzyme.

Furthermore, mitochondria expressing Psd1 devoid of the potential substrate recognition site showed no detectable decarboxylase activity. Also in this case impaired Psd1 processing into α - and β -subunits appears to be responsible for the observed effect. Thus, we can only speculate about the function of this domain as substrate recognition site. Our results rather indicate that SRS is responsible for protein stability and involved in autocatalytic processing.

4.4.2 Phospholipid distribution of wild type and Psd1 variants

The mitochondrial synthesis of PE in *Saccharomyces cerevisiae* is accomplished by decarboxylation of imported extramitochondrial PS by Psd1. Although a second decarboxylase (Psd2) is present in a Golgi/vacuole compartment, the majority of Psd1 activity is present in mitochondria. In order to investigate the influence of the predicted transmembrane domains and the potential substrate recognition site on the phospholipid distribution, phospholipids of the corresponding Psd1 mutants were extracted, isolated and quantified (Broekhuysse, 1986; Folch et al., 1957)

Tables 37-38 and Figures 28-29 show the results of the phospholipid determination of wild type Psd1, Psd1 Δ IM2, Psd1 Δ IM1+2 and Psd1 Δ SRS. Loss of enzymatic activity in Psd1 lacking the predicted transmembrane domains or the substrate recognition site, respectively, led to a typical *psd1* Δ phospholipid pattern displaying enrichment of PC at the expense of PE in mitochondria and homogenate. Thus, the phospholipid distribution reflects the impaired

autocatalytic processing of Psd1 Δ IM2, Psd1 Δ IM1+2 and Psd1 Δ SRS causing loss of enzymatic activity. Remaining PE in mitochondria was obviously synthesized by Psd2 and the acyltransferases Ale1 and Tgl3. As no ethanolamine was added to the growth media, the CDP-ethanolamine pathway (Kennedy pathway) may only contribute to PE biosynthesis through internal recycling of PC.

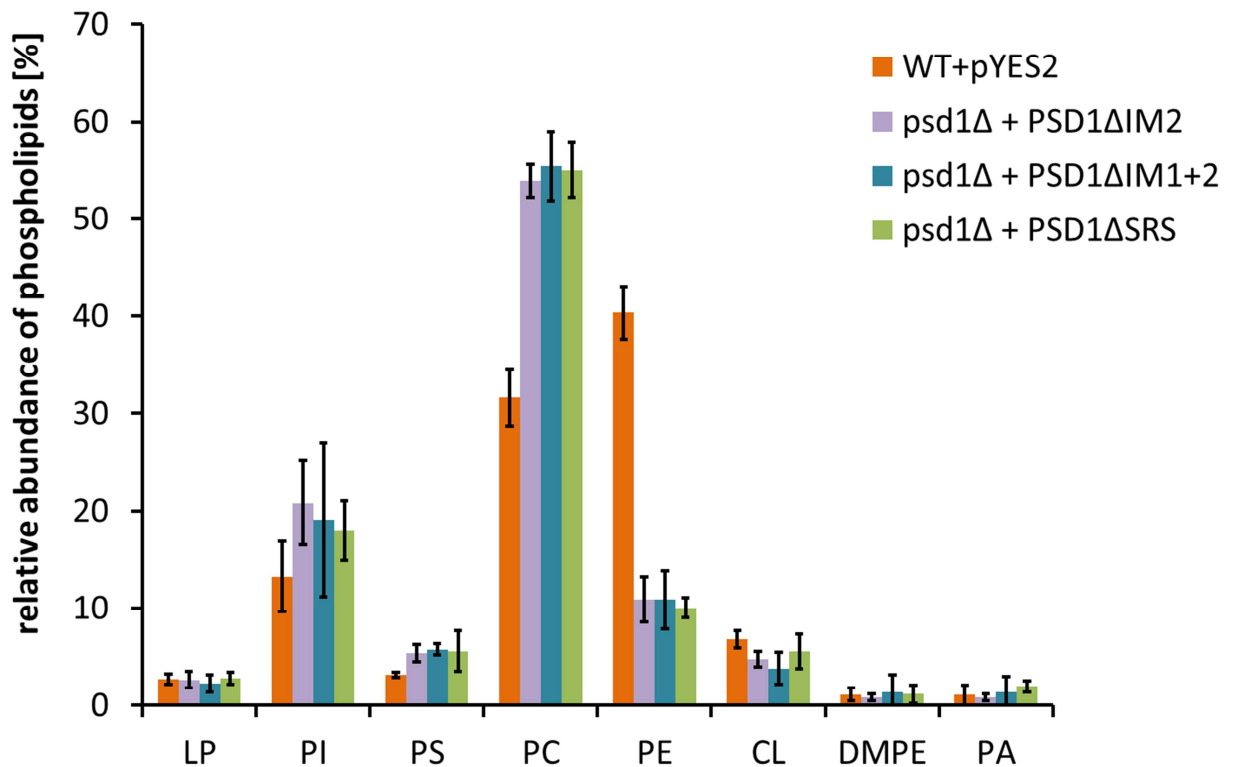


Figure 28: Phospholipid distribution in mitochondria of WT, Psd1 Δ IM2, Psd1 Δ IM1+2 and Psd1 Δ SRS

Table 37: Phospholipid distribution in mitochondria of WT, Psd1 Δ IM2, Psd1 Δ IM1+2 and Psd1 Δ SRS

	WT + pYES2	psd1 Δ + PSD1 Δ IM2	psd1 Δ + PSD1 Δ IM1+2	psd1 Δ +PSD1 Δ SRS
LP	2,70 ± 6	2,63 ± 0,8	2,26 ± 0,9	2,77 ± 0,6
PI	13,23 ± 3,6	20,81 ± 4,3	19,10 ± 8,0	17,98 ± 3,1
PS	3,12 ± 0,3	5,37 ± 0,9	5,76 ± 0,6	5,59 ± 2,1
PC	31,62 ± 3,0	53,89 ± 1,7	55,42 ± 3,6	55,01 ± 2,8
PE	40,33 ± 2,7	10,89 ± 2,3	10,87 ± 3,0	10,02 ± 1,0
CL	6,79 ± 0,9	4,75 ± 0,8	3,80 ± 1,6	5,52 ± 1,8
DMPE	1,14 ± 0,7	0,83 ± 0,3	1,40 ± 1,7	1,16 ± 0,9
PA	1,06 ± 1,1	0,84 ± 0,4	1,38 ± 1,6	1,95 ± 0,5

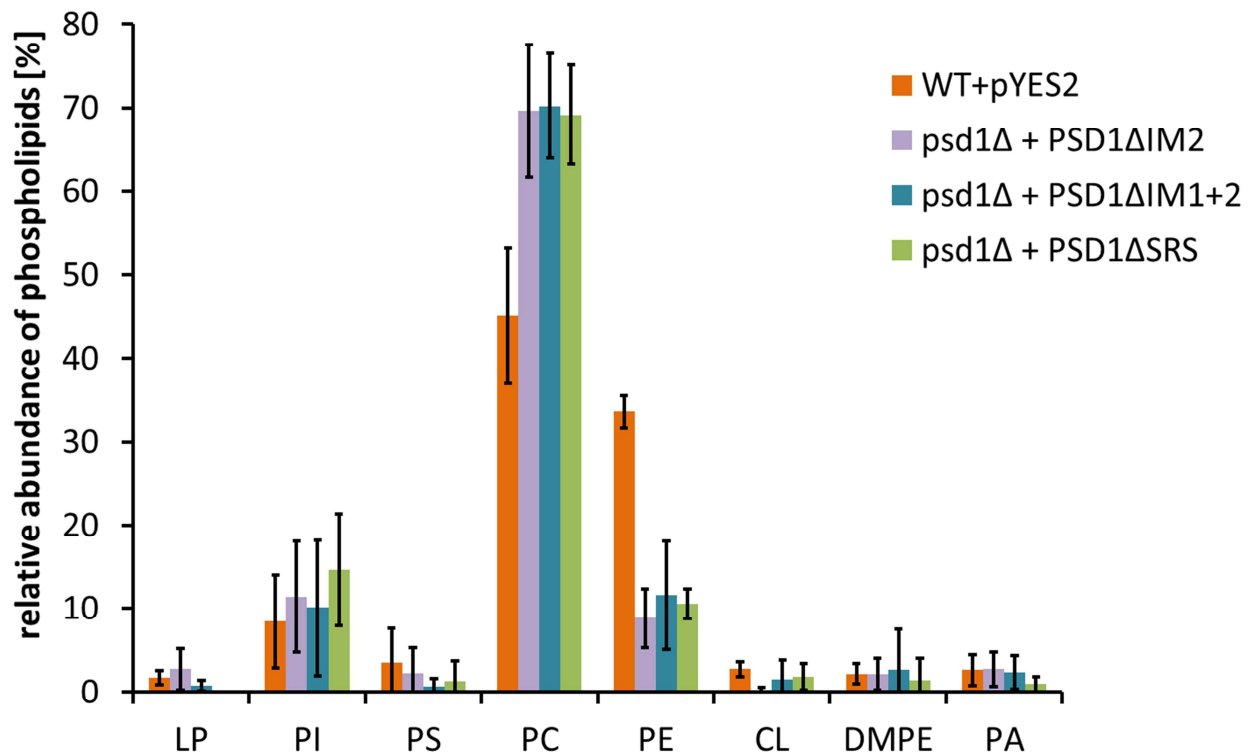


Figure 29: Phospholipid distribution in homogenate of WT, Psd1ΔIM2, Psd1ΔIM1+2 and Psd1ΔSRS

Table 38: Phospholipid distribution in homogenate of WT, Psd1ΔIM2, Psd1ΔIM1+2 and Psd1ΔSRS

	WT + pYES2	psd1Δ + PSD1ΔIM2	psd1Δ + PSD1ΔIM1+2	psd1Δ+PSD1ΔSRS
LP	1,73 ± 0,9	2,73 ± 2,5	0,81 ± 0,6	0
PI	8,48 ± 5,6	11,43 ± 6,6	10,10 ± 8,2	14,66 ± 6,7
PS	3,55 ± 4,1	2,26 ± 3,1	0,72 ± 0,9	1,36 ± 2,4
PC	45,06 ± 8,1	69,65 ± 7,9	70,23 ± 6,3	69,15 ± 5,9
PE	33,61 ± 1,91	8,84 ± 3,5	11,60 ± 6,5	10,56 ± 1,8
CL	2,76 ± 0,9	0,25 ± 0,3	1,55 ± 2,3	1,84 ± 1,6
DMPE	2,18 ± 1,2	2,10 ± 1,9	2,67 ± 4,9	1,46 ± 2,5
PA	2,63 ± 1,8	2,74 ± 2,1	2,32 ± 2,0	0,98 ± 0,9

5 Discussion

The majority of PE is synthesized by the mitochondrial Psd1 using PS as a substrate. The Psd1-precursor, which is synthesized on cytosolic ribosomes, contains N-terminal targeting sequences (MT) and an α - and a β -subunit which are linked by a highly conserved LGST motif (Figure 30) (Voelker, 1997).

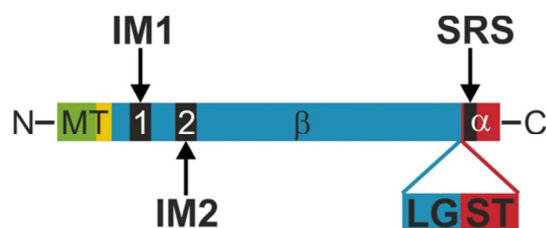


Figure 30: Psd1 domain structure displaying the predicted transmembrane domains (IM1 and IM2), the substrate recognition site (SRS), the LGST motif and the N-terminal targeting sequences (MT)

Upon import into mitochondria, posttranslational processing of Psd1 occurs in 3 proteolytic steps and gives rise to the mature and active form of the enzyme comprising an inner mitochondrial membrane bound β -subunit and a soluble α -subunit localized to the intermembrane space (Horvath et al., 2012). In addition, transmembrane domain prediction programs revealed two hydrophobic regions within the Psd1 β -subunit that may function as membrane anchors. Previous studies assigned IM1 to function as an anchor tethering Psd1 to the inner mitochondrial membrane.

A detailed characterization of the second predicted transmembrane domain (120-140 amino acids) and the potential substrate recognition site, homolog to that of CHO cells, should shed more light on Psd1 maturation and localization. In order to link specific functions of Psd1 to certain domains and motifs within the sequence and thereby getting more information about the mechanism(s) targeting Psd1 to the inner mitochondrial membrane/intermembrane space, a series of Psd1 variants lacking predicted

transmembrane domains (IM1, IM2) and the substrate recognition site (SRS) were cloned and subjected to biochemical analysis. Characterization of the respective mutants included localization studies, enzymatic analysis with radiolabeled substrates and phospholipid profiling.

It was demonstrated that Psd1 mutants lacking the second predicted transmembrane domain (IM2) showed an impairment of Psd1 processing into α - and β -subunits. The autocatalytic cleavage to α - and β -subunits is one of the most crucial steps in Psd1 processing and essential for the formation of the pyrovoyl prosthetic group, which is required for the activity of the enzyme (Voelker, 1997). Since Psd1 Δ IM2 and Psd1 Δ IM1+2 did not exhibit enzymatic activity, strains had a typical *psd1* Δ phospholipid pattern displaying an enrichment of PC at the expense of PE in mitochondria (Figure 28-29).

In addition, localization studies with Psd1 Δ IM2 and Psd1 Δ IM1+2 showed that Psd1 Δ IM2 is mislocalized to the outer mitochondrial membrane, whereas Psd1 Δ IM1+2 is mislocalized to the matrix (Figure 22). These findings provide two interesting aspects of Psd1 function. First, it suggests that the second predicted transmembrane domain (IM2) serves as internal mitochondrial targeting sequence and has no effect on anchoring the protein to membranes. Second, IM1 anchors the protein to the membrane and supports recently published data by Horvath et al. (2012).

It was demonstrated that Psd1 mutants lacking the first predicted transmembrane domain displayed a mislocalization to the matrix, which strongly indicates that IM1 functions as membrane anchor tethering Psd1 to the inner mitochondrial membrane. Moreover, it was shown that deletion of IM1 does not impair autocatalytic cleavage of the α - and β -subunit. Nevertheless, Psd1 Δ IM1 exhibits a decreased enzymatic activity and generates an altered

phospholipid pattern, displaying a slightly increased level of PC at the expense to PE in mitochondria. This slight reduction in the enzymatic activity is the result of mislocalization of Psd Δ IM1 to the mitochondrial matrix (Horvath et al., 2012).

Localization of Psd1 Δ IM2 to the outer mitochondrial membrane is another essential finding of this study. Since Psd1 Δ IM2 still contains the first predicted transmembrane domain which functions as membrane anchor, the enzyme is tethered to the outer mitochondrial membrane (Figure 22). The detailed mechanism of the incorporation of Psd1 Δ IM2 into the outer mitochondrial membrane has not yet been unveiled. However, it can be assumed that lack of the second predicted transmembrane domain (IM2) causes disruption of the Psd1 translocation process. Thus, it is likely that IM2 serves as internal targeting signal directing the Psd1-precursor to the inner mitochondrial membrane.

Interestingly, membrane integration studies of Psd1 Δ IM2/Psd1 Δ IM1+2 showed that deletion of IM1 increases the solubility but does not lead to a fully soluble protein. This result indicates that Psd1 mutants lacking the first predicted transmembrane domain and thus a membrane anchor are still associated with membranes. In contrast, deletion of the second predicted transmembrane domain does not influence protein solubility at all (Figure 25).

Previously, it was demonstrated that the matrix located peptidases Oct1 and MPP remove N-terminal mitochondrial targeting and sorting sequences from the Psd1-precursor during import into mitochondria (Horvath et al., 2012). For Psd1 Δ IM2 and Psd1 Δ IM1+2, N-terminal processing has not yet been investigated, but Western Blot analysis, indicated that both mutants are N-terminally processed. For Psd1 Δ IM2 and Psd1 Δ IM1+2 this might also be in a reaction catalyzed by Oct1 and MPP. In the case of Psd1 Δ IM1 the N-terminal processing by MPP and Oct1 has already been demonstrated.

Considering that the N-terminus of Psd1 Δ IM1 must be located to the mitochondrial matrix and deletion of IM1 causes partial solubility of Psd1, suggested the Psd1 model shown in Figure 32 (Horvath et al., 2012).

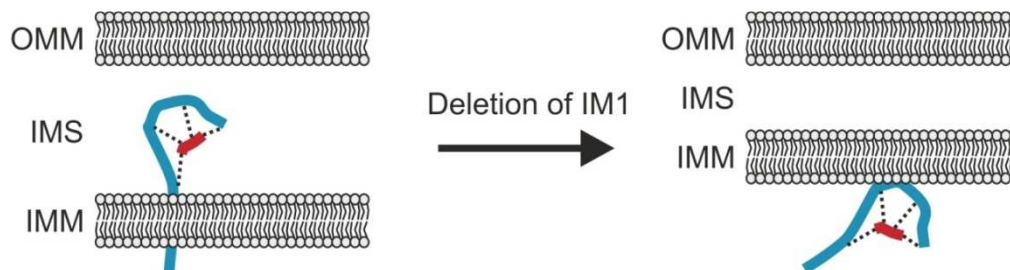


Figure 31: Localization of Psd1 upon deletion of IM1. Psd1, lacking IM1, is localized to the mitochondrial matrix and remains partially membrane bound.

Another consensus motif detected in phosphatidylserine decarboxylases, FXFXLKXXXXKXR, is found in CHO cells (amino acids 351-362) and in yeast Psd1 (amino acids 475-486) but not in *E. coli*. This motif is located to the α -subunit in near proximity to the catalytic carbonyl group and is thought to facilitate the specific interaction of the enzyme with the substrate PS (Igarashi et al., 1995; Schuiki and Daum, 2009).

To analyze the function of this domain, a Psd1 mutant lacking the substrate recognition site (SRS) was cloned and subjected to various biochemical analyses. Compared to the wild type Psd1, Psd1 Δ SRS exhibited no enzymatic activity, leading to a typical *psd1* Δ phospholipid pattern displaying an enrichment of PC at the expense of PE in mitochondria and homogenate (Figure 28-29). This finding does not indicate that the consensus motif within the α -subunit functions as substrate recognition site because Psd1 processing and stability were also impaired. Western blot analysis of Psd1 Δ SRS showed that deletion of SRS leads to depleted autocatalytic cleavage into α - and β -subunits and N-terminally degradation which include the antibody recognition site of Psd1 β . Topology and membrane integration of Psd1 Δ SRS revealed a mislocalization to the outer mitochondrial membrane.

In this study, specific functions of Psd1 could be linked to certain domains within the sequence. The first predicted transmembrane domain serves as membrane anchor tethering the protein to the inner mitochondria membrane (Horvath et al., 2012), whereas the second predicted transmembrane domain is involved in C-terminal processing and internal targeting. Moreover, it could be shown that the substrate recognition site of the α -subunits is responsible and essential for Psd1 processing and stability.

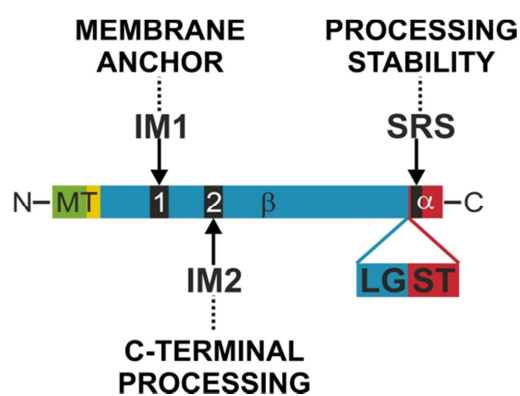


Figure 32: Overview of the specific functions of the hydrophobic regions (IM1 and IM2) and substrate recognition site (SRS)

7 References

- Achleitner, G., Zweytick, D., Trotter, P. J., Voelker, D. R. and Daum, G. (1995). Synthesis and intracellular transport of aminoglycerophospholipids in permeabilized cells of the yeast, *Saccharomyces cerevisiae*. *The Journal of Biological Chemistry* **270**, 29836-29842.
- Athenstaedt, K. and Daum G. (1999). Phosphatidic acid, a key intermediate in lipid metabolism. *European Journal of Biochemistry* **266**, 1-16.
- Baker, M. J., Frazier, A. E., Gulbis, J. M. and Rayn, M. T. (2007). Mitochondrial protein-import machinery: correlating structure with function. *Trends in Cell Biology* **17**, 457-464.
- Bauer, M. F., Hofmann, S. Neupert, W. and Brunner M. (2002). Protein translocation into mitochondria: the role of TIM complexes, *Trends in Cell Biology* **10**, 25-31.
- Birner R., Bürgermeister M., Schneiter R. and Daum G. (2001). Roles of phosphatidylethanolamine and of its several biosynthetic pathways in *Saccharomyces cerevisiae*. *Molecular Biology of the Cell* **12**, 997-1007.
- Böttinger L., Horvath, S. E., Kleinschroth T., Hunte, C., Daum, G., Pfanner, N. and Becker, T. (2012). Phosphatidylethanolamine and cardiolipin differentially affect the stability of mitochondrial respiratory chain supercomplexes. *Journal of Molecular Biology* **423**, 677–686.
- Broekhuysse, R. M. (1986). Phospholipids in tissues of the eye. Isolation, characterization, and quantitative analysis by two dimensional thin layer chromatography of diacyl and vinyl-ether phospholipids. *Biochemical and Biophysical Acta* **260**, 449-459.
- Cervený, K. L., McCaffery, J. M. and Jensen, R. E. (2001). Division of Mitochondria Requires a Novel *DNM1*-interacting Protein, Net2p. *Molecular Biology of the Cell* **12**, 309-321.
- Chacinska, A., Koehler, C. M., Milenkovic, D., Lithgow, T. and Pfanner N. (2009). Importing mitochondrial proteins: machineries and mechanisms. *Cell* **138**, 628-641.
- Christiansen, K., (1978) Triacylglycerol synthesis in lipid particles from baker's yeast (*Saccharomyces cerevisiae*). *Biochemical and Biophysical Acta* **530**, 78-90.
- Clancey, C. J., Chang, S.-C., and Dowhan, W. (1993). Cloning of a gene (PSD1) encoding phosphatidylserine decarboxylase from *Saccharomyces cerevisiae* by complementation of an *Escherichia coli* mutant. *The Journal of Biological Chemistry* **268**, 24580–24590.

Daum, G., Lees, N. D., Bard, M. and Dickson, R. (1998). Biochemistry, cell biology and molecular biology of lipids of *Saccharomyces cerevisiae*. *Yeast* **14**, 1471-1510.

Dean-Johnson, M. and Henry, S. A. (1989). Primary structure of myo-inositol -1-phosphate synthase (EC 5.5.1.4) and functional analysis of its structural gene, the INO1 locus. *The Journal of Biological Chemistry* **264**, 1274-1283.

Fahy, E., Subramaniam, S. and Brown, H. A. (2005). A comprehensive classification system for lipids. *Journal of Lipid Research* **46**, 839-861.

Fakas, S., Konstantinou, C. and Carman, G. M. (2011). DGK1-encoded diacylglycerol Kinase activity is required for phospholipid synthesis during growth resumption from stationary phase in *Saccharomyces cerevisiae*. *The Journal of Biological Chemistry* **286**, 1464-1474.

Fischl, A. S. and Carman, G. M. (1983). Phosphatidylinositol biosynthesis in *Saccharomyces cerevisiae*: purification and properties of microsome-associated phosphatidylinositol synthase. *Journal of Bacteriology* **154**, 304-311.

Frey, T. G. and Manella, C. A. (2000). The internal structure of mitochondria. *TIBS* **25**, 319-324.

Fruman, D. A., Meyers, R. E. and Cantley, L. C. (1998). Phosphoinositide kinases. *Annu Rev Biochem* **67**, 481-507.

Folch, J., Lees, M. and Sloane-Stanley, G. H. (1957). A simple method for isolation and purification of total lipids from animal tissues. *The Journal of Biological Chemistry* **226**, 497-509.

Gaigg B., Simbeni, R., Hrastnik, C., Paltauf, F. and Daum, G. (1994). Characterization of a microsomal subfraction associated with mitochondria of the yeast, *Saccharomyces cerevisiae*. Involvement in synthesis and import of phospholipids into mitochondria. *Biochimica et Biophysica Acta* **1234**, 214-220.

Gallet, P. F., Petit, J., Maftah, A., Zachowski, A. and Julien, R. (1997). Asymmetrical distribution of cardiolipin in yeast inner mitochondrial. *The Biochemical Journal* **324**, 627-634.

Gebert, N., Rayn, M. T., Pfanner, N., Wiedermann, N. and Stojanovski, D. (2011). Mitochondrial protein import machineries and lipids: a functional connection. *Biochemical and Biophysical Acta* **1808**, 1002-1011.

Gietz, D., St, J. A., Woods, R. A., and Schiestl, R. H. (1992). Improved method for high efficiency transformation of intact yeast cells. *Nucleic Acids Res.* **20**, 1425.

Griac, P. (1997). Regulation of yeast phospholipid biosynthetic genes in phosphatidylserine decarboxylase mutants. *Journal of Bacteriology* **179**, 5843-5848.

Hafez, I. M. and Cullis, P. R. (2001). Roles of lipid polymorphism in intracellular delivery. *Advanced Drug Delivery Reviews* **47**, 139-148.

Haid, A. and Suissa, M. (1983). Immunochemical identification of membrane proteins after sodium dodecyl sulphate-polyacrylamid gel electrophoresis. *Methods Enzymol.* **96**, 192-198.

Homann, M. J., Poole, M. A., Gaynor, P. M., Ho, C.-T. and Carman G. M. (1987). Effect of growth phase on phospholipid biosynthesis in *Saccharomyces cerevisiae*. *The Journal of Bacteriology* **169**, 533-539.

Horvath, S. E., Böttinger, L., Vögtle, F.-N., Wiedemann, N., Meisinger, C., Becker, T. and Daum, G. (2012). Processing and topology of the yeast mitochondrial phosphatidylserine decarboxylase 1. *The Journal of Biological chemistry* **287**, 36744-36755.

Igarashi, K., Kaneda, M., Yamaji, A., Saido, T. C., Kikkawa, U., Ono, Y. Inoue, K., and Umeda, M. (1995). A novel phosphatidylserine-binding peptide motif defined by an anti-idiotypic monoclonal antibody localization of phosphatidylserine-specific binding sites on protein kinase C and phosphatidylserine decarboxylase. *The Journal of Biological Chemistry* **270**, 29075-29078.

Jesch, S. A., Zhao, X., Wells, M. T. and Henry, S. A. (2005). Genome-wide analysis reveals inositol, not choline, as the major effector of Ino2p-Ino4p and unfolded protein response target gene expression in yeast. *The Journal of Biological Chemistry* **280**, 9106-9118.

Kitamura, H., Wu, W. I., and Voelker, D. R. (2002). The C2 domain of phosphatidylserine decarboxylase 2 is not required for catalysis but is essential for in vivo function. *The Journal of Biological Chemistry* **277**, 33720-33726.

Kornmann, B., Currie, E., Collins, S. R., Schuldiner, M., Nunnari, J., Weissman, J. S. and Walter P. (2009). An ER-mitochondria tethering complex revealed by a synthetic biology screen. *Science* **325**, 477-481.

Kuchler, K., Daum, G. and Paltauf, F. (1986). Subcellular and submitochondrial localization of phospholipid-synthesizing enzymes in *Saccharomyces cerevisiae*. *Journal of Bacteriology* **165**, 901-910.

Laemmli, U. K. (1970). Cleavage of structural proteins during the assembly of the head of Bacteriophage T4. *Nature* **227**, 680-685.

Lodish, H., Berk, A., Kaiser, C. A., Krieger, M., Scott, M. P. Bretscher, A., Ploegh, H. and Matsudaira, P. (2007). *Molecular Cell Biology/Sixth Edition*. W. H. Freeman and Company, New York.

Lopez, F., Leube, M., Gil-Mascarell, R., Navarro-Aviñó, J. P. and Serrano, R. (1999). The yeast inositol monophosphatase is a lithium- and sodium-sensitive enzyme encoded by a non-essential gene pair. *Molecular Microbiology* **31**, 1255-1264.

Lowry, O. H., Rosenbrough, N. J., Farr, A. L. and Rendell, R. J. (1951). Protein measurement with Folin phenol reagent. *The Journal of Biological Chemistry* **193**, 265-275.

Nebauer, R., Birner-Grünberger, R. and Daum G. (2004). Biogenesis and cellular dynamics of glycerophospholipids in yeast *Saccharomyces cerevisiae*. *Topics in Current Genetics* **6**, 125-168.

Nebauer, R., Schuiki, I., Kulterer, B., Trjanoski, Z. and Daum, G. (2007). The phosphatidylethanolamine level of yeast is affected by the mitochondrial components Oxa1p and Yme1p. *FEBS Journal* **274**, 6180-6190.

Nikawa, J., Tsukagoshi, Y. and Yamashita, S. (1991). Isolation and characterization of two distinct myo- inositol transporter genes of *Saccharomyces cerevisiae*. *The Journal of Biological Chemistry* **266**, 11184-11191.

Osman, C., Voelker, D. R. and Langer, T. (2011). Making heads or tails of phospholipids in mitochondria. *The Journal of Biological Chemistry* **192**, 7-16.

Otsuga, D., Keegan, B. R., Brisch, E., Thatcher, J. W., Hermann, G. J., Bleazard, W. and Shaw, J. M. (1998). The dynamin-related GTPase, Dnm1p, controls mitochondrial morphology in yeast. *Journal of Cell Biology* **143**, 344-349.

Pagac, M., Vazquez de la Mora, H., Duperrex, C., Roubaty, C., Vionnet, C. and Conzlmann, A. (2011). Topology of 1-acyl-sn-glycerol-3-phosphate acyltransferases *SLC1* and *ALE1* and related membrane-bound *O*-acyltransferases (MBOATs) of *Saccharomyces cerevisiae*. *The Journal of Biological Chemistry* **286**, 36438-36447.

Rajakumari, S. and Daum, G. (2010). Janus-faced enzymes yeast Tgl3p and Tgl5p catalyze lipase and acyltransferase reaction. *Molecular Biology of the Cell* **21**, 501-510.

Rajakumari, S., Grillitsch, K. and Daum, G. (2008). Synthesis and turnover of non-polar lipids in yeast. *Progress in Lipid Research* **47**, 157–171.

Riekhof, W. R., Wu, J., Jones, J. L. and Voelker D. R. (2007). Identification and characterization of the major lysophosphatidylethanolamine acyltransferase in *Saccharomyces cerevisiae*. *The Journal of Biological Chemistry* **282**, 28344-28352.

Schatz, G. (1996). The protein import system of mitochondria. *The Journal of Biological Chemistry* **271**, 31763-31766.

Schumacher, M. M., Choi, J.-Y. and Voelker, D. R. (2002). Phosphatidylserine transport to the mitochondria is regulated by ubiquitination. *The Journal of Biological Chemistry* **277**, 51033-51042.

Schuike, I. and Daum, G. (2009). Phosphatidylserine decarboxylases, key enzymes of lipid metabolism. *Life* **61**, 151-162.

Schuike, I., Schnabl, M., Czabany, T., Hrastnik, C. and Daum, G. (2010). Phosphatidylethanolamine synthesized by four different pathways is supplied to the plasma membrane of the yeast *Saccharomyces cerevisiae*. *Biochimica et Biophysica Acta* **1801**, 480-486.

Sorger, D. and Daum, G. (2003). Triacylglycerol biosynthesis in yeast. *Appl. Microbiol. Biotechnol.* **61**, 289-299.

Trotter, P. J., Pedretti, J. and Voelker, D. R. (1993). Phosphatidylserine decarboxylase from *Saccharomyces cerevisiae*. Isolation of mutants, cloning of the gene, and creation of a null allele. *Journal of Biological Chemistry* **268**, 21416–21424.

Trotter, P. J., Pedretti, J., Yates, R. and Voelker, D. R. (1995). Phosphatidylserine decarboxylase 2 of *Saccharomyces cerevisiae*. Cloning and mapping of the gene, heterologous expression, and creation of the null allele. *The Journal of Biological Chemistry* **270**, 6071–6080.

Tolias, K. F. and Cantley, L. C. (1999). Pathways for phosphoinositide synthesis. *Chemistry and Physics of Lipids* **98**, 69-77.

Tuller, G., Hrastnik, C., Achleitner, G., Schiefthaler, U., Klein, F. and Daum, G. (1998). YDL142c encodes cardiolipin synthase (Cls1p) and is non-essential for aerobic growth of *Saccharomyces cerevisiae*. *FEBS Letters* **421**, 15-18.

Tuller, G., Nemeč, T., Hraštnik, C. and Daum, G. (1999). Lipid composition of subcellular membranes of an FY1679-derived haploid yeast wild type strain grown on different carbon sources. *Yeast* **15**, 1555-1564.

Voelker, D. R. (1997). Phosphatidylserine decarboxylase, *Biochimica et Biophysica Acta* **1348**, 236-244.

Voet, D., Voet, J. G., Pratt, C. W. (2008). Principles of Biochemistry/ Third edition. John Wiley & Sons, Inc. Wiley-VHC Verlag GmbH & Co. KGaA, Weinheim.

Zinser, E. and Daum, G. (1995). Isolation and biochemical characterization of organelles from the yeast, *Saccharomyces cerevisiae*. *Yeast* **11**, 493-536.

8 Curriculum vitae

Personal Information

Name: Stefanie Horvath
Date of birth: 16th of October 1988
Place of birth: Graz, Austria
Citizenship: Austria

Education

1995-1999 Elementary School, Schulverein der Grazer Schulschwestern
1999-2003 Secondary School, Schulverein der Grazer Schulschwestern
2003-2007 Oberstufenrealgymnasium with additional/engrossed education in biology, chemistry und physics, Schulverein der Grazer Schulschwestern

Final examination (21th of June 2007)

2007-2011 Bachelor studies in Chemistry at Graz University of Technology
7/2010-9/2010 Bachelor thesis in the research group of Univ.-Prof. Dr.rer.nat. Peter Macheroux at the Institute of Biochemistry, Graz University of Technology

Conferment of the BSc academic degree (2th of February 2011)

Since 2011 Master studies of Biochemistry and Molecular Biomedicine at Graz University of Technology
11/2011-07/2012 Master thesis in the research group of Ao. Univ.-Prof. Dipl.-Ing. Dr.techn. Günther Daum at the Institute of Biochemistry, Graz University of Technology